Report

Current Biology

Human inbreeding has decreased in time through the Holocene

Highlights

- A study of 411 ancient genomes shows inbreeding decreased over time
- The decrease appears linked with population size increase enabled by agriculture
- Extreme consanguineous matings did occur among agriculturalists but were rare

Authors

Francisco C. Ceballos, Kanat Gürün, N. Ezgi Altınışık, ..., Füsun Özer, Çiğdem Atakuman, Mehmet Somel

Correspondence

somel.mehmet@gmail.com

In brief

Ceballos et al. study 411 ancient genomes from west and central Eurasia to show that overall inbreeding levels have decreased over time, most likely owing to population size increases with agriculture. The sample contains highly consanguineous ancient individuals, but these are rare, and all come from agriculturalist backgrounds.

Ceballos et al., 2021, Current Biology *31*, 3925–3934
September 13, 2021
https://doi.org/10.1016/j.cub.2021.06.027

CellPress

Current Biology

CellPress
OPEN ACCESS

Report

Human inbreeding has decreased in time through the Holocene

Francisco C. Ceballos,[1,7] Kanat Gürün,[1,7] N. Ezgi Altınışık,[2] Hasan Can Gemici,[3] Cansu Karamurat,[3] Dilek Koptekin,[1] Kıvılcım Başak Vural,[1] Igor Mapelli,[1] Ekin Sağlıcan,[1] Elif Sürer,[4] Yılmaz Selim Erdal,[2] Anders Götherström,[5,6] Füsun Özer,[2] Çiğdem Atakuman,[3] and Mehmet Somel[1,8,9,*]

[1]Department of Biological Sciences, Middle East Technical University, 06800 Ankara, Turkey
[2]Human-G Laboratory, Department of Anthropology, Hacettepe University, 06800 Ankara, Turkey
[3]Department of Settlement Archaeology, Middle East Technical University, 06800 Ankara, Turkey
[4]Department of Modeling and Simulation, Graduate School of Informatics, Middle East Technical University, 06800 Ankara, Turkey
[5]Department of Archaeology and Classical Studies, Stockholm University, Stockholm, Sweden
[6]Centre for Palaeogenetics, Svante Arrhenius väg 20C, 106 91 Stockholm, Sweden
[7]These authors have contributed equally
[8]Twitter: @CompEvoMetu
[9]Lead contact
*Correspondence: somel.mehmet@gmail.com
https://doi.org/10.1016/j.cub.2021.06.027

SUMMARY

The history of human inbreeding is controversial.[1] In particular, how the development of sedentary and/or agricultural societies may have influenced overall inbreeding levels, relative to those of hunter-gatherer communities, is unclear.[2–5] Here, we present an approach for reliable estimation of runs of homozygosity (ROHs) in genomes with ≥3× mean sequence coverage across >1 million SNPs and apply this to 411 ancient Eurasian genomes from the last 15,000 years.[5–34] We show that the frequency of inbreeding, as measured by ROHs, has decreased over time. The strongest effect is associated with the Neolithic transition, but the trend has since continued, indicating a population size effect on inbreeding prevalence. We further show that most inbreeding in our historical sample can be attributed to small population size instead of consanguinity. Cases of high consanguinity were rare and only observed among members of farming societies in our sample. Despite the lack of evidence for common consanguinity in our ancient sample, consanguineous traditions are today prevalent in various modern-day Eurasian societies,[1,35–37] suggesting that such practices may have become widespread within the last few millennia.

RESULTS AND DISCUSSION

To study runs of homozygosity (ROH) levels in time, we tailored the *PLINK* implementation of ROH calling to suit relatively low-coverage ancient genomes. Simulations using *in silico*-generated ancient DNA reads with spiked-in ROH showed that *PLINK* calls ROHs accurately down to 5× coverage. We also observed that at 3× coverage, or with 30% SNP missingness rates, *PLINK* calls tend to deviate from expected values in the number of ROH > 1Mb (*NROH*) and the sum of ROH > 1Mb (*SROH*) (Data S1A) (Data S1, S2, and S3 can be found at Zenodo Data: https://doi.org/10.5281/zenodo.4906173). We next performed simulations using empirical data by downsampling n = 44 relatively high coverage (>10×) ancient genomes. This showed that in real data, the default *PLINK* algorithm overestimates *NROH* and *SROH* at 3× coverage due to missed heterozygous positions in the data (Figure S1; Table S1). We could empirically account for this bias by varying the parameters of *PLINK* with respect to the number of heterozygous SNP allowed per window conditional on coverage, and we could thus estimate *NROH* and *SROH* > 1Mb reliably for ≥3× coverage genomes in downsampling simulations (Figures S2A and S2B; STAR Methods). Meanwhile, we found that ROH < 1Mb cannot be identified reliably at low coverage, and therefore we did not include such short ROHs in downstream analyses (STAR Methods).

Using our conditional approach for ROH calling, we estimated ROHs in 411 published ancient genomes that either had ≥3× mean SNP coverage or had ≥2× coverage and <30% missing SNPs across the 1240K SNP set[6] (Data S1B; STAR Methods). We further compared our approach with alternative tools for ROH inference. Recently, two model-based ROH inference algorithms have been reported for ancient genomes. That of Renaud and colleagues,[38] *ROHan*, was shown to infer ROH reliably down to 5× coverage, while Ringbauer and colleagues' method, *hapROH*,[39] infers ROH > 4 Mb from genomes down to 0.3× coverage, taking advantage of a modern haplotype reference panel. We compared our approach with *hapROH* across the 384 genomes covered in both studies and found high correlations (R^2 > 0.81 and 0.89, respectively) for both *NROH* and *SROH* values (STAR Methods).

Our analyses below focus on ROH > 1Mb estimated across the aforementioned 411 genomes, as well as among 448 contemporary human individuals (Figures S3A and S3B). We focused on West Eurasia (Europe) and Central Eurasia (SW Asia, Caucasus,

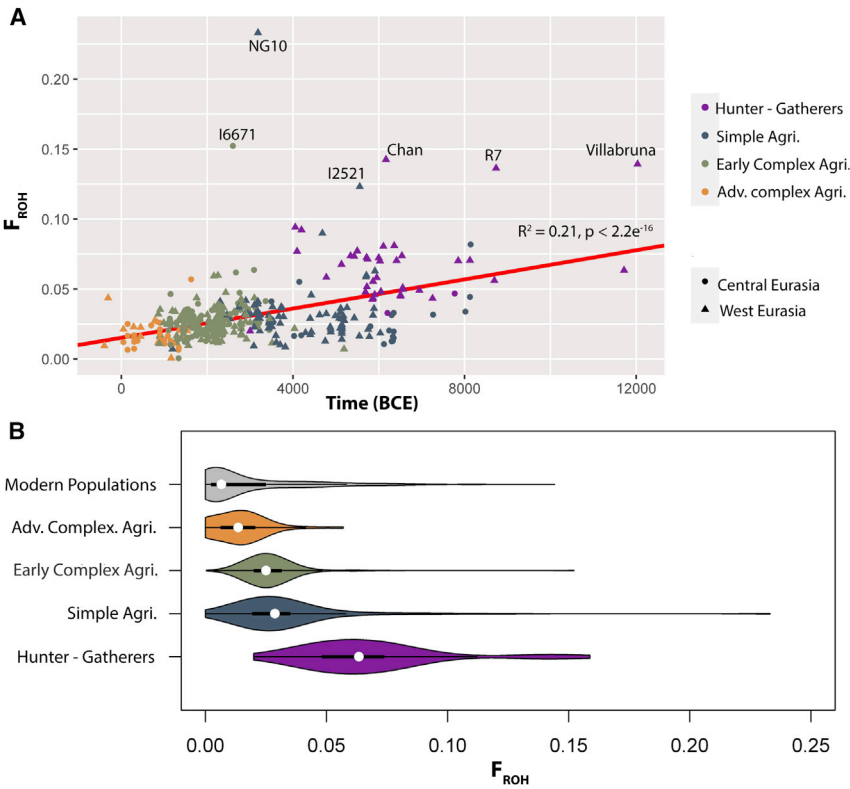

Figure 1. Temporal distribution of the genomic inbreeding coefficient (F_{ROH})

(A) Regression of F_{ROH} estimates against time (sample age) in years Before Common Era (BCE). Cultural groups are defined with colors: "hunter-gatherers" in violet, "simple agriculturalists" (Simple Agri.) in blue, "early complex agriculturalists" (Early Complex Agri.) in green, "advanced complex agriculturalists" (Adv. Complex Agri.) in orange, and present-day populations from the Human Genome Diversity Panel in gray. The region of origin of each individual is shown with a symbol: Central Eurasia with a circle and West Eurasia with a triangle. The regression line was obtained by analyzing only the ancient individuals (n = 411) and has a significant slope (Pearson adjusted $R^2 = 0.21$, $p < 2e^{-16}$).

(B) Violin plots of F_{ROH} estimates for the different cultural groups and modern-day populations from the Human Genome Diversity Panel. In addition, in multiple regression analysis that includes sample archaeological age and cultural groupings together, we found that sample age has a significant contribution to the full model (Data S3, adjusted $R^2 = 0.32$, $p < 2e^{-16}$), while the effect of each cultural grouping was also significant in comparison to the baseline set by the hunter-gatherers (simple agriculturalists' $p = 5e^{-10}$; early complex agriculturalists' $p = 2e^{-15}$; and advanced complex agriculturalists' $p = 3e^{-08}$). In addition, comparing the F_{ROH} distributions between pairs of groups, all comparisons were highly nominally significant (Wilcoxon rank sum test $p < 1e^{-10}$; Data S1D) except for the comparisons involving simple agriculturalists versus early complex agriculturalists, and that involving advanced complex agriculturalists versus modern-day populations ($p > 0.09$).

and Central Asia), regions with the highest published ancient genome data density. To study the effects of varying social and economic organization on inbreeding among Holocene populations, we separated past societies into four broad cultural groups based on their subsistence and mobility patterns that are historically contingent for each region (see "Classification into broad cultural groups" in STAR Methods): "hunter-gatherers," who subsisted on wild resources within egalitarian mobile bands (e.g., Gravettian hunter-gatherers in East Europe[40]); "simple agriculturalists," the earliest adopters of agriculture within relatively egalitarian sedentary communities (e.g., Linearbandkeramik farmers of Central Europe[41–43]); "early complex agriculturalists," farmer/pastoralist communities with emerging institutionalized hierarchy and specialization (e.g., Bell Beaker groups known mainly from burials in West and Central Europe[44–46]); and "advanced complex agriculturalists," living in highly stratified societies organized around state systems (e.g., the Roman state in the Mediterranean[47]). We note that these do not represent simple temporal categories and may cross-cut different millennia in different regions (Data S1C).[48–50]

Temporal and spatial distribution of human inbreeding

We first studied the temporal distribution of autozygosity, i.e., homozygosity created by inbreeding, in West and Central Eurasia. We used F_{ROH}, the genomic inbreeding coefficient, as a measure of autozygosity, estimated as *SROH* > 1.5Mb per genome.[51] We find a manifest trend of decreasing levels of autozygosity over time in Eurasia through the Holocene (Figure 1A). When separating the data into five broad cultural groups, from hunter-gatherers to advanced complex agriculturalists and finally to contemporary humans, we observe the same trend. Notably, the largest shift in F_{ROH} occurs between hunter-gatherers and simple agriculturalists, during the Neolithic transition, but the trend is sustained in later periods (Data S1D).

We next studied the spatial distribution of F_{ROH}. Notably, the distribution of F_{ROH} is highly structured in present-day Eurasia (Figure S3B; Table 1). In contrast, we found that temporal changes in F_{ROH} were largely consistent across different regions of Eurasia: neither a multiple regression analysis, with latitude and longitude as dependent variables ($\beta_{latitude} = 2.1e^{-04}$, $p = 0.181$; $\beta_{longitude} = 8.9e^{-06}$, $p = 0.789$), nor kriging analysis (Figure 2) revealed any prominent spatial structure for F_{ROH} through different cultural groupings. We also noted that contemporary populations have the lowest average inbreeding levels, despite high variability within this group (Figure 1B; Table 1).

Given the heterogeneity of this sample with respect to genome coverage and missing SNP proportions (Figures S2E and S2F), we further studied whether these technical factors may influence the above observations. Both coverage and missingness values showed weak but sometimes significant correlations with sample archaeological age and F_{ROH} (STAR Methods; Table S2). We, therefore, performed three additional tests to assess possible effects of technical variation on the above results. First, we carried out multiple regression analyses with F_{ROH} as the

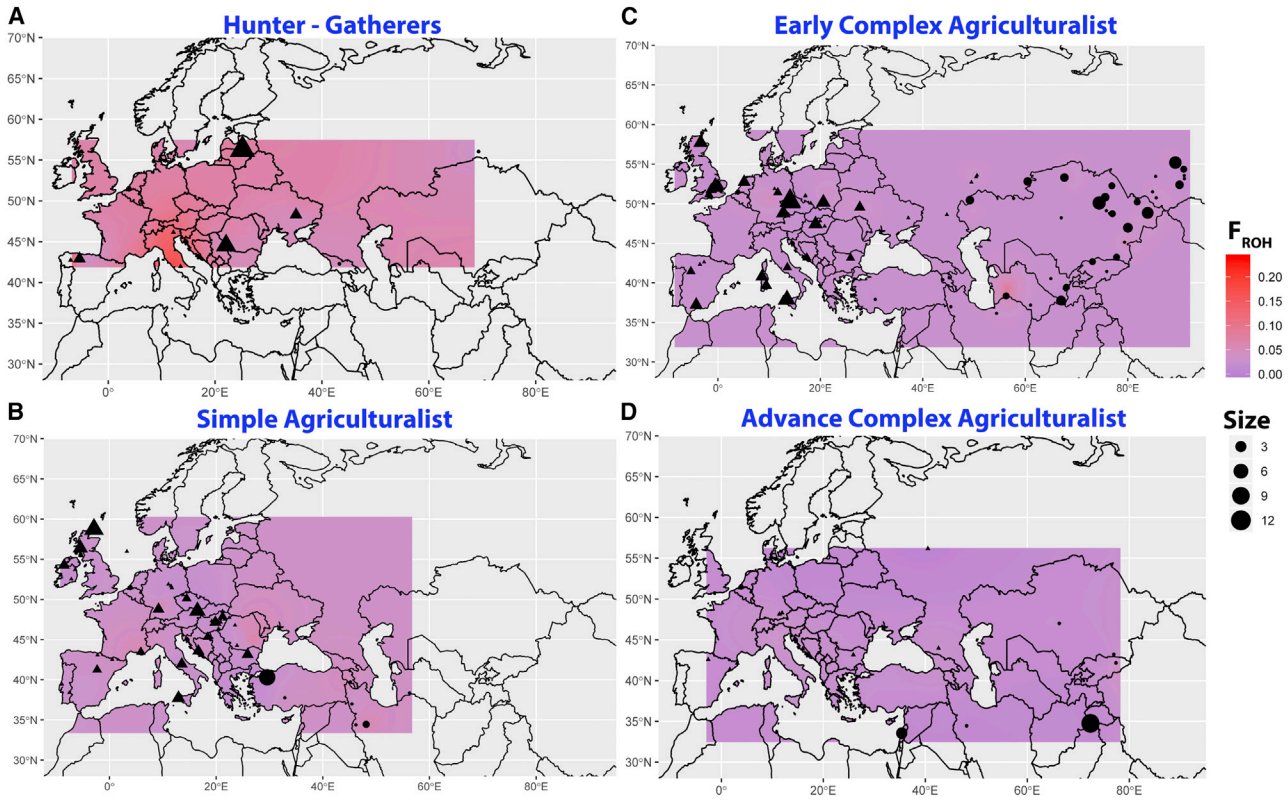

Figure 2. Spatially kriged reconstructions for the distribution of the genomic inbreeding coefficient (F_{ROH})

The colors represent the predicted F_{ROH} values. The panels show spatial kriging of F_{ROH} estimates in hunter-gatherers (A), in the simple agriculturalists (B), in the early complex agriculturalists (C), and in the advanced complex agriculturalists (D). See also Data S1A.

dependent variable and archaeological age, cultural grouping, coverage (measured in two different ways), and missingness as independent variables (see "Testing the effects of varying coverage" in STAR Methods and Data S3). We found that the coverage and missingness have no significant influence on the estimated F_{ROH} levels in this model. Second, we repeated F_{ROH} estimation after downsampling all 411 genomes to 3× coverage and testing the effects of time, cultural grouping, and space on these F_{ROH} estimates (Figures S2H–S2J). Third, we repeated F_{ROH} estimation by calling ROH using a >1.9 M SNP panel ascertained in 1000 Genomes Project Yoruba individuals[52] and using 72 shotgun-sequenced individuals (see "The effect of using a denser SNP panel" in STAR Methods and Figures S2H–S2J). Our results in both experiments confirmed that neither variation in genome coverages within our sample nor SNP panel choice could explain the observed decrease in F_{ROH} with time.

The origins of autozygosity in ancient humans

We find extreme autozygosity in some ancient individuals within our dataset (Figure 1A). Autozygosity can be caused by two distinct but non-exclusive processes:[53] (1) panmictic inbreeding, which is produced by genetic drift in isolated populations and will be stronger with smaller population size, and (2) systematic inbreeding, which is produced by deviations from panmixia, as occurs with cultural consanguinity in humans (see STAR Methods). Throughout the rest of the manuscript, we refer to these processes as drift and consanguinity, respectively. The contributions of drift and consanguinity to autozygosity can be studied qualitatively by comparing *NROH* versus *SROH* per individual genome. Strong drift creates proportionately high *NROH* and *SROH*. Conversely, consanguinity creates mainly long ROH, and thus, disproportionately high *SROH* relative to *NROH*.[54]

Using this approach, we explored the origins of extreme autozygosity signals in our data. In Figure 3, the diagonal line is set by an outbred population with no evidence of consanguinity[54] (STAR Methods). Individuals with high values along the diagonal exhibit high autozygosity due to drift, while "right shifts" from the diagonal indicate consanguinity (Figure S4). We observe that autozygosity among our sample of 411 ancient individuals can be mostly attributed to drift caused by small population size. Most notably, individuals assigned to the hunter-gatherer category, with overall high F_{ROH} levels, revealed no obvious indication of consanguinity. This included some West Eurasian hunter-gatherers with extreme autozygosity ($F_{ROH} > 0.125$; Chan, Villabruna, and R7). The vast majority of agriculturalists likewise showed no evidence of consanguinity. Within the agriculturalist sample, however, the three individuals with the most extreme autozygosity ($F_{ROH} > 0.125$) displayed the right shift that indicates consanguinity. We compared the *NROH* and *SROH* observed in these individuals with the values expected under different types of consanguinity in simulations (see "Consanguineous mating

Table 1. Summary statistics for the genomic inbreeding coefficient calculated from ROHs (F_{ROH}) across broad cultural groupings and geographical regions

	N	Median F_{ROH}	IQC	$F > 0.0117$		$F > 0.0391$		$F > 0.0932$	
				N	%	N	%	N	%
Hunter-gatherers	40	0.0633	0.026	40	100	38	92.6	4	9.7
West Eurasia	38	0.0687	0.026	38	100	37	97.3	4	10.5
Central Eurasia	2	0.0397	0.006	2	100	1	50.0	0	0.0
Simple agriculturalists	102	0.0286	0.014	97	95.1	15	14.7	2	1.9
West Eurasia	83	0.0290	0.012	79	95.2	11	13.3	2	2.4
Central Eurasia	19	0.0201	0.017	18	94.7	4	21.1	0	0.0
Early complex agriculturalists	230	0.0250	0.011	221	96.0	15	6.5	1	0.4
West Eurasia	145	0.0241	0.010	138	95.1	7	4.8	0	0.0
Central Eurasia	85	0.0269	0.011	83	97.6	8	9.4	1	1.2
Advanced complex agriculturalists	39	0.0160	0.009	30	76.9	2	5.1	0	0.0
West Eurasia	9	0.0212	0.006	7	77.7	1	11.1	0	0.0
Central Eurasia	30	0.0151	0.006	23	76.7	1	3.3	0	0.0
Human Genome Diversity Panel	448	0.0066	0.022	172	38.4	74	16.5	6	1.3
West Eurasia	139	0.0039	0.005	19	13.7	3	2.2	0	0.0
Central Eurasia	309	0.0156	0.034	153	49.5	71	23.0	6	1.9

N, number of individuals; IQC, interquartile range; $F > 0.0117$, individuals with $F_{ROH} > 0.0117$ (individuals who could be offspring of second cousin matings or closer matings); $F > 0.039$, individuals with $F_{ROH} > 0.039$ (individuals who could be offspring of first cousin matings or closer matings, ignoring drift); $F > 0.093$, number and percentage of individuals with $F_{ROH} > 0.093$ (individuals who could be offspring of avuncular matings or closer matings, ignoring drift).

simulations" in STAR Methods). We thus estimate that individual NG10 from Middle Neolithic Ireland (3338–3028 cal BCE) may be the offspring of an incest mating (brother-sister or parent-offspring), as suggested by Cassidy and colleagues[7] (Figure 3B; Figure S4). We further estimate that individuals I6671 from Early-Middle Bronze Age Turkmenistan (3000–2039 cal BCE) and I2521 from Neolithic Bulgaria (5619–5491 cal BCE) may be the offspring of avuncular matings (uncle-niece, aunt-nephew, or double first cousins), while also exhibiting additional autozygosity due to drift.

We further studied the distribution of ROHs using the total length of ROH values for different ROH track lengths (Figure 3C). The size of ROHs is inversely correlated with its age: longer ROHs are inherited from recent common ancestors, while shorter ROHs come from distant ancestors, broken down by recombination. We found that among those hunter-gatherer individuals with extreme autozygosity, total lengths of short ROHs (between 1 and 2 Mb) are high, implicating autozygosity by drift. Conversely, among ancient genomes from food producing societies, the three with the highest autozygosity, NG10, I6671, and I2521, have high levels of long ROHs (ROH > 8 Mb) total lengths, indicating consanguinity. The individual NG10 reveals five ROHs of size > 30 Mb, with an estimated age of just one generation.[57] Overall, consanguinity appears rare, with only three (0.7%) of all ancient individuals analyzed exhibiting strong evidence for consanguinity.

We finally repeated the *NROH* versus *SROH* comparison using ancient genomes downsampled to 3× coverage. Our *PLINK*-based conditional approach tends to underestimate consanguinity at 3× coverage due to overestimation of *NROH*, but the three most consanguineous individuals identified with the original data (NG10, I6671, and I2521) are still identified as outliers (Figure S2I). This result, as well as qualitatively similar conclusions reached in an independent study,[39] confirm that consanguinity explains only a small fraction of the overall autozygosity observed.

The origins of present-day autozygosity in Central Eurasia

We then studied the spatial distribution of present-day inbreeding prevalence in relation to ancient inbreeding patterns. Figure 3D presents the average sum of the different ROH sizes across regions and cultural groupings. This reveals an interesting spatiotemporal structure, especially for the shorter ROHs (1–2 Mb) in Figure 3D. West Eurasian hunter-gatherers carry the highest total length of short ROHs among all historical groups, attesting to their small population size around the early Holocene, as recently inferred using high-quality ancient genomes.[58] However, this inbreeding signal is rapidly lost, and West Eurasian advanced agriculturalists carry the lowest average sum of short ROHs among all ancient groups studied. In Central Eurasia, the total length of short ROHs is also high in hunter-gatherers and decreases in agriculturalists, but at a more modest rate (*SROH* decreases from c.235.3 Mb to c.85.1 Mb in West Eurasia, and from c.168.3 Mb to c.115.5 Mb in Central Eurasia). Compared to ancient populations, present-day populations have the shortest average total length of shorter ROHs, denoting large effective population size and slow genetic drift.

However, this temporal pattern vanishes when we study the total length of longer ROHs, e.g., ROHs between 4 and 8 Mb. Importantly, ROH > 4 Mb may have an age of 5 to 10 generations[37,51,59] and thus indicate relatively close consanguinity. Figure 3D reveals that some modern-day Central Eurasian populations (e.g., Balochi of Pakistan or the Bedouin from Saudi

Arabia) carry higher total lengths of ROHs between 4 and 8 Mb than any other group in the HGDP dataset, as well as any of our historical cultural groupings.

In Table 1, we present comparisons of median F_{ROH} and the frequency of individuals with high autozygosity. As also observed in Figure 3, we find that present-day populations tend to carry the lowest proportions of individuals with high F_{ROH}. However, some present-day Eurasian groups have exceptionally high proportions of individuals with $F_{ROH} > 0.0391$ (i.e., individuals who could be offspring of first cousin matings or closer matings, ignoring drift; STAR Methods). This is especially salient among certain Central Eurasian populations. Samples from modern groups like the Balochi, the Bedouin, or the Sindhi from Pakistan have the highest proportions of individuals with $F_{ROH} > 0.0391$ (50%, 41.3%, and 33.3% respectively).

Comparing contemporary Central versus West Eurasia with respect to the proportion of individuals with high autozygosity, we find a significant difference between the two regions, both for individuals with $F_{ROH} > 0.0391$ (odds ratio = 13.5, Fisher's exact test $p = 9e^{-10}$) and also for individuals with $F_{ROH} > 0.0117$ (i.e., individuals who could be offspring of second cousin matings or closer matings, ignoring drift) (odds ratio = 6.2, $p = 7e^{-14}$) (Table 1). Because Central Eurasian populations also exhibit relatively high total lengths of long ROH, this excess of individuals with high autozygosity could be attributed to consanguinity, rather than drift-related processes such as caste endogamy. This result is consistent with documented cultural preferences for first-cousin matings in some contemporary societies.[60,61]

This raises the question of whether the differential rates of consanguinity among present-day Central versus West Eurasia could be traced back in time. In fact, we observed an excess of individuals with $F_{ROH} > 0.0117$ in Central versus West Eurasia among "advanced complex agriculturalists," roughly spanning third to first millennium BC, depending on region (odds ratio = 5.1, p = 0.009; Table 1; Data S1C). However, we find no indication that this difference was driven by consanguinity, i.e., excess of long ROHs, in these ancient societies (Figure 3). Consequently, high rates of consanguinity in Central Eurasia observed today might have only a recent history.

Conclusion

The impact of food production and social complexity on human inbreeding levels has been an open question. One plausible effect is sedentism and food surplus allowing population growth[2] and thus leading to weaker drift and diminished autozygosity. On the other hand, the advent of private property in food producing societies could have promoted the role of biological kinship in the group; consequently, customs such as consanguineous marriage or caste endogamy[3,36] could have elevated overall autozygosity. The net impact of these potential demographic and cultural processes on autozygosity has remained unknown.

Our results demonstrate that the Neolithic transition to agriculture and the emergence of complex societies led to significantly lower levels of overall autozygosity in both West and Central Eurasia. This could have been driven by food production-driven population growth, as well as elevated rates of population admixture as inferred from archaeogenomic data.[8,62] These processes must have mitigated total autozygosity by reducing the strength of drift throughout recent history.

Of course, here we rely on the assumption that the 411 individuals analyzed in this study were representative of their time. Sampling biases caused by various factors, such as the burial location of the elite versus the commoners, or a focus on elite burials by archaeologists, could influence inferences on class-based societies. That said, the fact that our data derive from 181 different archaeological sites, and also our observation that autozygosity decreases in parallel both in West and in Central Eurasia, lend support to our conclusions. We further note that our results are consistent with previous work. Earlier ROH analyses of single genomes have suggested that high levels of drift-driven autozygosity were common in the genomes of hunter-gatherers from Upper Paleolithic and Mesolithic periods from Europe and the Caucasus.[5,9] A recent report that used model-based ROH inference on ancient genomes also identified a temporal decrease in >4 Mb ROH levels across global human populations, similar to the trend described here.[39]

Three points further deserve mention regarding mating patterns in human societies. One is the seeming contrast between the high levels of drift-driven autozygosity (panmictic inbreeding) we report for ancient hunter-gatherer societies and ethnographic studies showing low levels of inbreeding among modern-day hunter-gatherers. For instance, a comparison of inbreeding patterns in a worldwide sample of contemporary hunter-gatherers with Amazonian horticulturalists reported lower inbreeding in hunter-gatherer groups.[3] Hill and colleagues also report low levels of relatedness within modern-day hunter-gatherer bands.[4] However, the mentioned ethnographic findings rely on genealogies and report the prevalence of inbreeding by consanguinity, not inbreeding by drift. In fact, we also find consanguinity to be rare among early Holocene Eurasian hunter-gatherers relative to agriculturalists, consistent with widespread exogamy in modern-day hunter-gatherers. This raises the possibility that reciprocal exogamy and consanguinity avoidance traditions may have been predominant among human foragers since prehistory (but possibly not in archaic hominins[63]).

Second, our results lend support, albeit with limited data, to the hypothesis that extreme consanguinity may have become more common with farming. This result parallels higher within-group marriages among modern-day horticulturalists than foragers.[3] It is also consistent with singular reports on ancient agriculturalist genomes, such as evidence for consanguinity identified in an early Neolithic farmer from Iran,[10] a first-degree incest case from Neolithic Ireland,[7] as well as a recent report on close-kin unions in the central Andes after 1000 CE.[64] In our analysis, among the seven individuals with the highest level of inbreeding (with $F_{ROH} > 0.125$), all four hunter-gatherers appear autozygous by drift, while all three agriculturalists appear autozygous by consanguinity. This appears unlikely to happen by chance (Fisher's exact test, two-sided p = 0.029). These results are consistent with the view that consanguineous traditions could have thrived in class-based agricultural societies with private property more readily than in more egalitarian hunter-gatherer groups.

Finally, we report higher consanguinity in Central versus West Eurasia in contemporary societies, in parallel with earlier work.[35] This is consistent with widespread first- or second-cousin marriage practices in agricultural societies in Middle Eastern and North African countries and in South Asia,

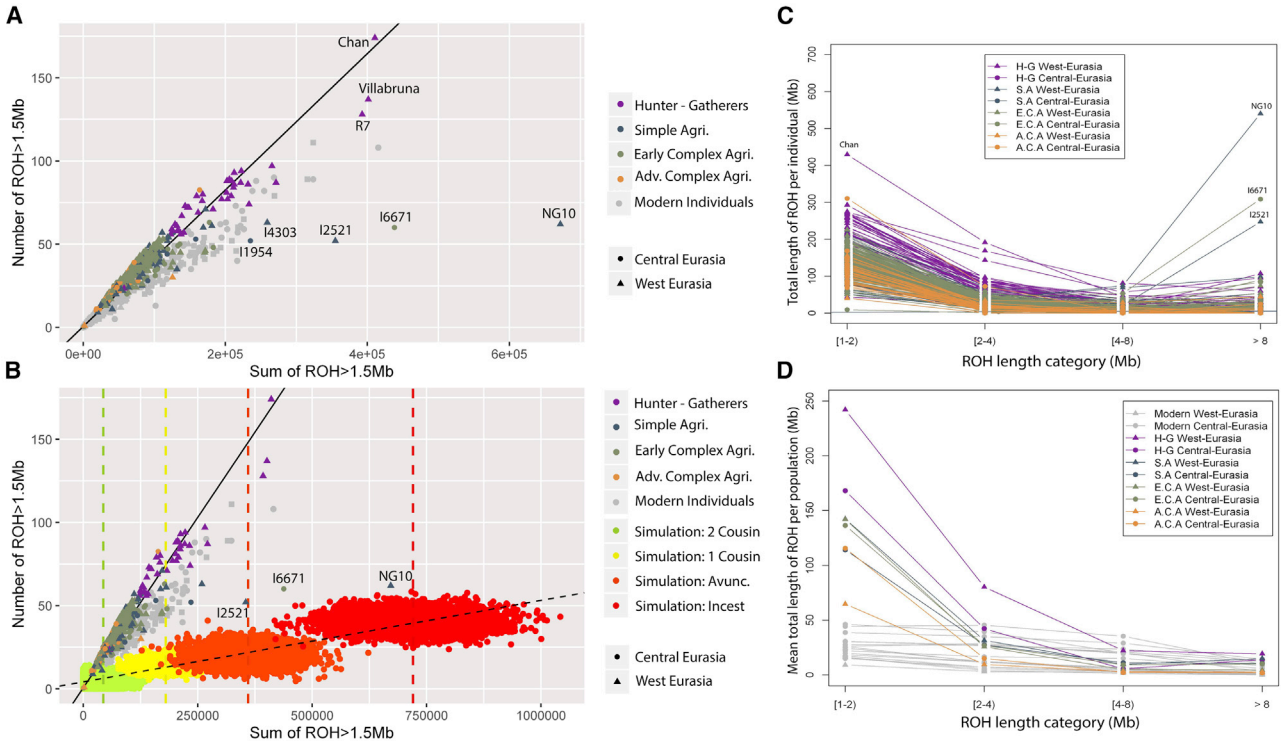

Figure 3. Assessing ROH origins

(A) Mean number of ROHs and sum of ROHs, for ROH > 1.5 Mb, is plotted for each individual. The diagonal line is obtained by the regression of the number of ROH versus the sum of ROH in ASW and ACB populations from the 1000 Genomes Project that represent admixed and thus relatively outbred populations.[55,56] Consanguinity practices in the previous generation are visible as a right shift in this figure.

(B) Simulations of the number and sum of ROHs, for ROH > 1.5 Mb, calculated for the offspring of different consanguineous matings are shown, along with the ancient and modern samples. Points with different colors designate offspring of different consanguineous mating: second cousin (green), first cousin (yellow), avuncular (uncle-niece, aunt-nephew, double first cousin) (orange), incest (brother-sister, parent-offspring) (red). Five thousand simulations are represented for each consanguineous mating (see STAR Methods). Note that this simulation does not include drift, but the degree of right shift can be projected to cases where there exists a non-zero level of autozygosity due to drift. Vertical lines represent the average sum of ROHs (>1.5Mb) for the offspring of each type of consanguineous mating. We also present results for a similar simulation of consanguinity using genotype data from two modern-day populations (ASW and CHS) in Figure S2G and for a simulation of consanguinity and drift together for chromosome 1 in Figure S4.

(C) The total length of ROHs (Mb) over four classes of ROH tract lengths: $1 \leq \text{ROH} < 2$ Mb, $2 \leq \text{ROH} < 4$ Mb, $4 \leq \text{ROH} < 8$ Mb, and $\text{ROH} \geq 8$ Mb, described for each ancient individual. Individuals were colored according to region and cultural groupings: West Eurasia hunter-gatherers (H-G West-Eurasia, shown in purple triangles), Central Eurasian hunter-gatherers (H-G Central-Eurasia shown in purple circles), West Eurasia simple agriculturalists (S.A West-Eurasia shown in blue triangles), Central Eurasian simple agriculturalists (S.A Central-Eurasia shown in blue circles), West Eurasia early complex agriculturalists (E.C.A West-Eurasia shown in green triangles), Central Eurasian early complex agriculturalists (E.C.A Central-Eurasia shown in green circles), West Eurasia advanced complex agriculturalists (A.C.A West-Eurasia shown in yellow triangles), Central Eurasian advanced complex agriculturalists (A.C.A Central-Eurasia shown in yellow circles).

(D) The total length of ROHs (Mb) over four classes of ROH tract lengths as in (C), calculated as the average for the different groups of individuals. The coloring scheme is the same as in (C); in addition, modern-day populations are represented in gray triangles (modern West-Eurasian populations) and circles (modern Central-Eurasian populations).

including Muslim and Jewish groups, as documented by ethnographic or genomic studies.[1,36,60,65] We note that cousin marriages were also common among royal dynasties and upper classes of Europe until the 20th century, and many prominent European scientists of that period are known to have married their first cousins, including Charles Darwin and Albert Einstein.[66,67] These traditions are thought to have arisen through various social factors, including the inheritance of property in class societies.[1,3,68] Interestingly, we do not observe the relatively high rates of consanguineous marriage observed in modern-day Central Eurasia in any of the past societies we studied, in Antiquity or earlier. We naturally prefer to remain cautious, especially given the limited sample size of our advanced complex agriculturalist samples from West and Central Eurasia (n = 9 and n = 30, respectively). Nevertheless, it appears possible that present-day cultural patterns may have emerged relatively late in time.

STAR★METHODS

Detailed methods are provided in the online version of this paper and include the following:

- KEY RESOURCES TABLE
- RESOURCE AVAILABILITY
  - Lead contact

SUPPLEMENTAL INFORMATION

Supplemental information can be found online at https://doi.org/10.1016/j.cub.2021.06.027.

ACKNOWLEDGMENTS

We are grateful to the METU CompEvo group, Torsten Günther, Liisa Loog, and three anonymous reviewers for helpful suggestions and/or comments, Harald Ringbauer for sharing unpublished results and discussion, Jim Wilson and David Clark for support, and the David Reich lab and all archaeogenomic groups who have shared their data used in this work. This work was supported by the ERC Consolidator Grant "NEOGENE" (no. 772390 to M.S.) and TÜBITAK of Turkey (no. 117Z229 to M.S.).

AUTHOR CONTRIBUTIONS

F.C. and M.S. conceived and designed the study; F.C.C., K.G., and K.B.V. analyzed genetic data, with contributions from D.K., M.S., I.M., and E. Sağlıcan; H.C.G., C.K., and Ç.A. determined the cultural groupings with contributions by Y.S.E.; M.S. supervised the study with contributions by N.E.A., Ç.A., E. Sürer, Y.S.E., A.G., and F.Ö.; F.C.C., K.G., M.S., and N.E.A. wrote the manuscript with contributions from all authors.

DECLARATION OF INTERESTS

The authors declare no competing interests.

Received: September 23, 2020
Revised: April 19, 2021
Accepted: June 10, 2021
Published: July 2, 2021

REFERENCES

1. Bittles, A.H., and Black, M.L. (2010). Evolution in health and medicine Sackler colloquium: Consanguinity, human evolution, and complex diseases. Proc. Natl. Acad. Sci. USA *107* (*Suppl 1*), 1779–1786.
2. Gignoux, C.R., Henn, B.M., and Mountain, J.L. (2011). Rapid, global demographic expansions after the origins of agriculture. Proc. Natl. Acad. Sci. USA *108*, 6044–6049.
3. Walker, R.S. (2014). Amazonian horticulturalists live in larger, more related groups than hunter-gatherers. Evol. Hum. Behav. *35*, 384–388.
4. Hill, K.R., Walker, R.S., Bozicević, M., Eder, J., Headland, T., Hewlett, B., Hurtado, A.M., Marlowe, F., Wiessner, P., and Wood, B. (2011). Co-residence patterns in hunter-gatherer societies show unique human social structure. Science *331*, 1286–1289.
5. Sikora, M., Seguin-Orlando, A., Sousa, V.C., Albrechtsen, A., Korneliussen, T., Ko, A., Rasmussen, S., Dupanloup, I., Nigst, P.R., Bosch, M.D., et al. (2017). Ancient genomes show social and reproductive behavior of early Upper Paleolithic foragers. Science *358*, 659–662.
6. Mathieson, I., Lazaridis, I., Rohland, N., Mallick, S., Patterson, N., Roodenberg, S.A., Harney, E., Stewardson, K., Fernandes, D., Novak, M., et al. (2015). Genome-wide patterns of selection in 230 ancient Eurasians. Nature *528*, 499–503.
7. Cassidy, L.M., Maoldúin, R.Ó., Kador, T., Lynch, A., Jones, C., Woodman, P.C., Murphy, E., Ramsey, G., Dowd, M., Noonan, A., et al. (2020). A dynastic elite in monumental Neolithic society. Nature *582*, 384–388.
8. Kılınç, G.M., Omrak, A., Özer, F., Günther, T., Büyükkarakaya, A.M., Bıçakçı, E., Baird, D., Dönertaş, H.M., Ghalichi, A., Yaka, R., et al. (2016). The Demographic Development of the First Farmers in Anatolia. Curr. Biol. *26*, 2659–2666.
9. Jones, E.R., Gonzalez-Fortes, G., Connell, S., Siska, V., Eriksson, A., Martiniano, R., McLaughlin, R.L., Gallego Llorente, M., Cassidy, L.M., Gamba, C., et al. (2015). Upper Palaeolithic genomes reveal deep roots of modern Eurasians. Nat. Commun. *6*, 8912.
10. Broushaki, F., Thomas, M.G., Link, V., López, S., van Dorp, L., Kirsanow, K., Hofmanová, Z., Diekmann, Y., Cassidy, L.M., Díez-Del-Molino, D., et al. (2016). Early Neolithic genomes from the eastern Fertile Crescent. Science *353*, 499–503.
11. Amorim, C.E.G., Vai, S., Posth, C., Modi, A., Koncz, I., Hakenbeck, S., La Rocca, M.C., Mende, B., Bobo, D., Pohl, W., et al. (2018). Understanding 6th-century barbarian social organization and migration through paleogenomics. Nat. Commun. *9*, 3547.
12. Lipson, M., Szécsényi-Nagy, A., Mallick, S., Pósa, A., Stégmár, B., Keerl, V., Rohland, N., Stewardson, K., Ferry, M., Michel, M., et al. (2017). Parallel palaeogenomic transects reveal complex genetic history of early European farmers. Nature *551*, 368–372.
13. Mathieson, I., Alpaslan-Roodenberg, S., Posth, C., Szécsényi-Nagy, A., Rohland, N., Mallick, S., Olalde, I., Broomandkhoshbacht, N., Candilio, F., Cheronet, O., et al. (2018). The genomic history of southeastern Europe. Nature *555*, 197–203.
14. Narasimhan, V.M., Patterson, N., Moorjani, P., Rohland, N., Bernardos, R., Mallick, S., Lazaridis, I., Nakatsuka, N., Olalde, I., Lipson, M., et al. (2019). The formation of human populations in South and Central Asia. Science *365*, eaat7487.
15. de Barros Damgaard, P., Martiniano, R., Kamm, J., Moreno-Mayar, J.V., Kroonen, G., Peyrot, M., Barjamovic, G., Rasmussen, S., Zacho, C., Baimukhanov, N., et al. (2018). The first horse herders and the impact of early Bronze Age steppe expansions into Asia. Science *360*, eaar7711.
16. Fu, Q., Posth, C., Hajdinjak, M., Petr, M., Mallick, S., Fernandes, D., Furtwängler, A., Haak, W., Meyer, M., Mittnik, A., et al. (2016). The genetic history of Ice Age Europe. Nature *534*, 200–205.
17. Gamba, C., Jones, E.R., Teasdale, M.D., McLaughlin, R.L., Gonzalez-Fortes, G., Mattiangeli, V., Domboróczki, L., Kővári, I., Pap, I., Anders, A., et al. (2014). Genome flux and stasis in a five millennium transect of European prehistory. Nat. Commun. *5*, 5257.
18. Günther, T., Malmström, H., Svensson, E.M., Omrak, A., Sánchez-Quinto, F., Kılınç, G.M., Krzewińska, M., Eriksson, G., Fraser, M., Edlund, H., et al. (2018). Population genomics of Mesolithic Scandinavia: Investigating early postglacial migration routes and high-latitude adaptation. PLoS Biol. *16*, e2003703.
19. Haak, W., Lazaridis, I., Patterson, N., Rohland, N., Mallick, S., Llamas, B., Brandt, G., Nordenfelt, S., Harney, E., Stewardson, K., et al. (2015).

Massive migration from the steppe was a source for Indo-European languages in Europe. Nature *522*, 207–211.

20. Lazaridis, I., Patterson, N., Mittnik, A., Renaud, G., Mallick, S., Kirsanow, K., Sudmant, P.H., Schraiber, J.G., Castellano, S., Lipson, M., et al. (2014). Ancient human genomes suggest three ancestral populations for present-day Europeans. Nature *513*, 409–413.
21. Allentoft, M.E., Sikora, M., Sjögren, K.G., Rasmussen, S., Rasmussen, M., Stenderup, J., Damgaard, P.B., Schroeder, H., Ahlström, T., Vinner, L., et al. (2015). Population genomics of Bronze Age Eurasia. Nature *522*, 167–172.
22. Fernandes, D.M., Mittnik, A., Olalde, I., Lazaridis, I., Cheronet, O., Rohland, N., Mallick, S., Bernardos, R., Broomandkhoshbacht, N., Carlsson, J., et al. (2020). The spread of steppe and Iranian-related ancestry in the islands of the western Mediterranean. Nat. Ecol. Evol. *4*, 334–345.
23. Hofmanová, Z., Kreutzer, S., Hellenthal, G., Sell, C., Diekmann, Y., Díez-Del-Molino, D., van Dorp, L., López, S., Kousathanas, A., Link, V., et al. (2016). Early farmers from across Europe directly descended from Neolithic Aegeans. Proc. Natl. Acad. Sci. USA *113*, 6886–6891.
24. Lazaridis, I., Mittnik, A., Patterson, N., Mallick, S., Rohland, N., Pfrengle, S., Furtwängler, A., Peltzer, A., Posth, C., Vasilakis, A., et al. (2017). Genetic origins of the Minoans and Mycenaeans. Nature *548*, 214–218.
25. Mittnik, A., Wang, C.C., Pfrengle, S., Daubaras, M., Zariņa, G., Hallgren, F., Allmäe, R., Khartanovich, V., Moiseyev, V., Tõrv, M., et al. (2018). The genetic prehistory of the Baltic Sea region. Nat. Commun. *9*, 442.
26. Olalde, I., Mallick, S., Patterson, N., Rohland, N., Villalba-Mouco, V., Silva, M., Dulias, K., Edwards, C.J., Gandini, F., Pala, M., et al. (2019). The genomic history of the Iberian Peninsula over the past 8000 years. Science *363*, 1230–1234.
27. Sánchez-Quinto, F., Malmström, H., Fraser, M., Girdland-Flink, L., Svensson, E.M., Simões, L.G., George, R., Hollfelder, N., Burenhult, G., Noble, G., et al. (2019). Megalithic tombs in western and northern Neolithic Europe were linked to a kindred society. Proc. Natl. Acad. Sci. USA *116*, 9469–9474.
28. Schroeder, H., Margaryan, A., Szmyt, M., Theulot, B., Włodarczak, P., Rasmussen, S., Gopalakrishnan, S., Szczepanek, A., Konopka, T., Jensen, T.Z.T., et al. (2019). Unraveling ancestry, kinship, and violence in a Late Neolithic mass grave. Proc. Natl. Acad. Sci. USA *116*, 10705–10710.
29. Veeramah, K.R., Rott, A., Groß, M., van Dorp, L., López, S., Kirsanow, K., Sell, C., Blöcher, J., Wegmann, D., Link, V., et al. (2018). Population genomic analysis of elongated skulls reveals extensive female-biased immigration in Early Medieval Bavaria. Proc. Natl. Acad. Sci. USA *115*, 3494–3499.
30. González-Fortes, G., Jones, E.R., Lightfoot, E., Bonsall, C., Lazar, C., Grandal-d'Anglade, A., Garralda, M.D., Drak, L., Siska, V., Simalcsik, A., et al. (2017). Paleogenomic Evidence for Multi-generational Mixing between Neolithic Farmers and Mesolithic Hunter-Gatherers in the Lower Danube Basin. Curr. Biol. *27*, 1801–1810.e10.
31. Günther, T., Valdiosera, C., Malmström, H., Ureña, I., Rodriguez-Varela, R., Sverrisdóttir, Ó.O., Daskalaki, E.A., Skoglund, P., Naidoo, T., Svensson, E.M., et al. (2015). Ancient genomes link early farmers from Atapuerca in Spain to modern-day Basques. Proc. Natl. Acad. Sci. USA *112*, 11917–11922.
32. Haber, M., Doumet-Serhal, C., Scheib, C.L., Xue, Y., Mikulski, R., Martiniano, R., Fischer-Genz, B., Schutkowski, H., Kivisild, T., and Tyler-Smith, C. (2019). A Transient Pulse of Genetic Admixture from the Crusaders in the Near East Identified from Ancient Genome Sequences. Am. J. Hum. Genet. *104*, 977–984.
33. Olalde, I., Brace, S., Allentoft, M.E., Armit, I., Kristiansen, K., Booth, T., Rohland, N., Mallick, S., Szécsényi-Nagy, A., Mittnik, A., et al. (2018). The Beaker phenomenon and the genomic transformation of northwest Europe. Nature *555*, 190–196.
34. Olalde, I., Schroeder, H., Sandoval-Velasco, M., Vinner, L., Lobón, I., Ramirez, O., Civit, S., García Borja, P., Salazar-García, D.C., Talamo, S., et al. (2015). A common genetic origin for early farmers from mediterranean cardial and central european LBK cultures. Mol. Biol. Evol. *32*, 3132–3142.
35. Bittles, A.H. (2012). Consanguinity in context. In Consanguinity in Context (Cambridge University Press), pp. 225–231.
36. Marchi, N., Mennecier, P., Georges, M., Lafosse, S., Hegay, T., Dorzhu, C., Chichlo, B., Ségurel, L., and Heyer, E. (2018). Close inbreeding and low genetic diversity in Inner Asian human populations despite geographical exogamy. Sci. Rep. *8*, 9397.
37. Ceballos, F.C., Joshi, P.K., Clark, D.W., Ramsay, M., and Wilson, J.F. (2018). Runs of homozygosity: windows into population history and trait architecture. Nat. Rev. Genet. *19*, 220–234.
38. Renaud, G., Hanghøj, K., Korneliussen, T.S., Willerslev, E., and Orlando, L. (2019). Joint estimates of heterozygosity and runs of homozygosity for modern and ancient samples. Genetics *212*, 587–614.
39. Ringbauer, H., Novembre, J., and Steinrücken, M. (2020). Human Parental Relatedness through Time - Detecting Runs of Homozygosity in Ancient DNA. bioRxiv. https://doi.org/10.1101/2020.05.31.126912.
40. Gamble, C. (1999). The Palaeolithic Societies of Europe, Second Edition (Cambridge University Press).
41. Czerniak, L. (2013). House, household and village in the Early Neolithic of central Europe: a case study of the LBK in Little Poland. In Environment and Subsistence - forty years after Janusz Kruk's. In Settlement studies, S. Kadrow, and P. Włodarczak, eds. (Dr. Rudolf Habelt GmbH), pp. 43–67.
42. Hachem, L., and Hamon, C. (2014). Linear Pottery Culture Household Organisation. An Economic Model. In Early farmers: The view from Archaeology and Science, A. Whittle, and P. Bickle, eds. (Oxford University Press), pp. 159–180.
43. Coudart, A. (1991). Social Structure and Relationships in Prehistoric Small-Scale Sedentary Societies: The Bandkeramik Groups in Neolithic Europe. In Between Bands and States, S.A. Gregg, ed. (Southern Illinois University), pp. 395–420.
44. Garrido-Pena, R. (2006). Transegalitarian societies: an ethnoarchaeological model for the analysis of Copper Age Bell Beaker using groups in Central Iberia. In Social Inequality in Iberian Late Prehistory, P. Díaz-del-Río, and L. García Sanjuán, eds. (Archaeopress), pp. 81–96.
45. Makarowicz, P.M. (2015). Personal Identity and Social Structure of Bell Beakers: The Upper Basins of the Oder and Vistula Rivers. In The Bell Beaker Transition in Europe: Mobility and Local Evolution during the 3rd Millennium BC, P.P. Martinez, and L. Salanova, eds. (Oxbow Books), pp. 15–27.
46. Salanova, L. (2016). Behind the warriors: Bell Beakers and identities in Atlantic Europe (Third Millennium B.C.). In Celtic from the West 3: Atlantic Europe in the Metal Ages — questions of shared language, K. Cleary, and C.D. Gibson, eds. (Oxbow Books), pp. 13–39.
47. Finley, M.I. (1974). The Ancient Economy (University of California Press).
48. Milisauskas, S. (2011). European prehistory: A survey, Second Edition (Springer Science & Business Media).
49. C. Renfrew, and P. Bahn, eds. (2014). The Cambridge World Prehistory (Cambridge University Press).
50. A. Yasur-Landau, E.H. Cline, and Y. Rowan, eds. (2018). The Social Archaeology of the Levant (Cambridge University Press).
51. McQuillan, R., Leutenegger, A.L., Abdel-Rahman, R., Franklin, C.S., Pericic, M., Barac-Lauc, L., Smolej-Narancic, N., Janicijevic, B., Polasek, O., Tenesa, A., et al. (2008). Runs of homozygosity in European populations. Am. J. Hum. Genet. *83*, 359–372.
52. Auton, A., Brooks, L.D., Durbin, R.M., Garrison, E.P., Kang, H.M., Korbel, J.O., Marchini, J.L., McCarthy, S., McVean, G.A., and Abecasis, G.R.; 1000 Genomes Project Consortium (2015). A global reference for human genetic variation. Nature *526*, 68–74.
53. Templeton, A.R., and Read, B. (1994). Inbreeding: one word, several meanings, much confusion. EXS *68*, 91–105.

54. Ceballos, F.C., Hazelhurst, S., and Ramsay, M. (2018). Assessing runs of Homozygosity: a comparison of SNP Array and whole genome sequence low coverage data. BMC Genomics *19*, 106.

55. Ceballos, F.C., Hazelhurst, S., and Ramsay, M. (2019). Runs of homozygosity in sub-Saharan African populations provide insights into complex demographic histories. Hum. Genet. *138*, 1123–1142.

56. Sudmant, P.H., Rausch, T., Gardner, E.J., Handsaker, R.E., Abyzov, A., Huddleston, J., Zhang, Y., Ye, K., Jun, G., Fritz, M.H.Y., et al.; 1000 Genomes Project Consortium (2015). An integrated map of structural variation in 2,504 human genomes. Nature *526*, 75–81.

57. Yengo, L., Wray, N.R., and Visscher, P.M. (2019). Extreme inbreeding in a European ancestry sample from the contemporary UK population. Nat. Commun. *10*, 3719.

58. Marchi, N., Winkelbach, L., Schulz, I., Brami, M., Hofmanová, Z., Blöcher, J., Reyna-Blanco, C.S., Diekmann, Y., Thiéry, A., Kapopoulou, A., et al. (2020). The mixed genetic origin of the first farmers of Europe. bioRxiv. https://doi.org/10.1101/2020.11.23.394502.

59. Kirin, M., McQuillan, R., Franklin, C.S., Campbell, H., McKeigue, P.M., and Wilson, J.F. (2010). Genomic runs of homozygosity record population history and consanguinity. PLoS ONE *5*, e13996.

60. Kang, J.T.L., Goldberg, A., Edge, M.D., Behar, D.M., and Rosenberg, N.A. (2016). Consanguinity Rates Predict Long Runs of Homozygosity in Jewish Populations. Hum. Hered. *82*, 87–102.

61. Jalkh, N., Sahbatou, M., Chouery, E., Megarbane, A., Leutenegger, A.L., and Serre, J.L. (2015). Genome-wide inbreeding estimation within Lebanese communities using SNP arrays. Eur. J. Hum. Genet. *23*, 1364–1369.

62. Lazaridis, I., Nadel, D., Rollefson, G., Merrett, D.C., Rohland, N., Mallick, S., Fernandes, D., Novak, M., Gamarra, B., Sirak, K., et al. (2016). Genomic insights into the origin of farming in the ancient Near East. Nature *536*, 419–424.

63. Prüfer, K., Racimo, F., Patterson, N., Jay, F., Sankararaman, S., Sawyer, S., Heinze, A., Renaud, G., Sudmant, P.H., de Filippo, C., et al. (2014). The complete genome sequence of a Neanderthal from the Altai Mountains. Nature *505*, 43–49.

64. Ringbauer, H., Steinrücken, M., Fehren-Schmitz, L., and Reich, D. (2020). Increased rate of close-kin unions in the central Andes in the half millennium before European contact. Curr. Biol. *30*, R980–R981.

65. Scott, E.M., Halees, A., Itan, Y., Spencer, E.G., He, Y., Azab, M.A., Gabriel, S.B., Belkadi, A., Boisson, B., Abel, L., et al.; Greater Middle East Variome Consortium (2016). Characterization of Greater Middle Eastern genetic variation for enhanced disease gene discovery. Nat. Genet. *48*, 1071–1076.

66. Ceballos, F.C., and Álvarez, G. (2013). Royal dynasties as human inbreeding laboratories: the Habsburgs. Heredity *111*, 114–121.

67. Álvarez, G., Ceballos, F.C., and Berra, T.M. (2015). Darwin was right: inbreeding depression on male fertility in the Darwin family. Biol. J. Linn. Soc. Lond. *114*, 474–483.

68. Korotayev, A. (2000). Parallel-cousin (FBD) marriage, Islamization, and Arabization. Ethnology *39*, 395–407.

69. Li, H., and Durbin, R. (2009). Fast and accurate short read alignment with Burrows-Wheeler transform. Bioinformatics *25*, 1754–1760.

70. Li, H., Handsaker, B., Wysoker, A., Fennell, T., Ruan, J., Homer, N., Marth, G., Abecasis, G., and Durbin, R.; 1000 Genome Project Data Processing Subgroup (2009). The Sequence Alignment/Map format and SAMtools. Bioinformatics *25*, 2078–2079.

71. Kircher, M. (2012). Analysis of high-throughput ancient DNA sequencing data. Methods Mol. Biol. *840*, 197–228.

72. Jun, G., Wing, M.K., Abecasis, G.R., and Kang, H.M. (2015). An efficient and scalable analysis framework for variant extraction and refinement from population-scale DNA sequence data. Genome Res. *25*, 918–925.

73. Li, H. (2011). A statistical framework for SNP calling, mutation discovery, association mapping and population genetical parameter estimation from sequencing data. Bioinformatics *27*, 2987–2993.

74. Chang, C.C., Chow, C.C., Tellier, L.C.C.A.M., Vattikuti, S., Purcell, S.M., and Lee, J.J. (2015). Second-generation PLINK: rising to the challenge of larger and richer datasets. Gigascience *4*, 7.

75. Purcell, S., and Chang, C. (2015). PLINK.

76. Renaud, G., Hanghøj, K., Willerslev, E., and Orlando, L. (2017). gargammel: a sequence simulator for ancient DNA. Bioinformatics *33*, 577–579.

77. Caballero, M., Seidman, D.N., Qiao, Y., Sannerud, J., Dyer, T.D., Lehman, D.M., Curran, J.E., Duggirala, R., Blangero, J., Carmi, S., and Williams, A.L. (2019). Crossover interference and sex-specific genetic maps shape identical by descent sharing in close relatives. PLoS Genet. *15*, e1007979.

78. Kelleher, J., Etheridge, A.M., and McVean, G. (2016). Efficient Coalescent Simulation and Genealogical Analysis for Large Sample Sizes. PLoS Comput. Biol. *12*, e1004842.

79. D.T. Price, and G. Feinman, eds. (2012). Pathways to power: New perspectives on the emergence of social inequality (Springer).

80. Richerson, P.J., and Boyd, R. (1999). Complex societies : The evolutionary origins of a crude superorganism. Hum. Nat. *10*, 253–289.

81. Scheidel, W. (2013). Studying the State. In The Oxford Handbook of the State in the Ancient Near East and Mediterranean, P.F. Bang, and W. Scheidel, eds. (Oxford University Press).

82. Shennan, S.J. (1999). The development of rank societies. In Companion Encyclopedia of Archaeology, G. Barker, ed. (Routledge), pp. 870–907.

83. Arnold, J.E. (1996). The archaeology of complex hunter-gatherers. J. Archaeol. Method Theory *3*, 77–126.

84. Renfrew, C., and Bahn, P.G. (2016). Archaeology: theories, methods and practice, Seventh Edition (Thames & Hudson).

85. Hayden, B. (2014). Social complexity. In The Oxford handbook of the archaeology and anthropology of hunter-gatherers, , V. Cummings, P. Jordan, and M. Zvelebil, eds. (Oxford University Press), pp. 643–662.

86. Bar-Yosef, O., and Belfer-Cohen, A. (2000). Nahal Ein Gev II - A Late Epi-Paleolithic Site in the Jordan Valley. J. Israel Prehist. Soc. *30*, 49–71.

87. Simmons, A.H. (2011). The neolithic revolution in the near east: Transforming the human landscape (University of Arizona Press).

88. Souvatzi, S.G. (2008). A Social Archaeology of Households in Neolithic Greece: An Anthropological Approach (Cambridge University Press).

89. Stoddart, S. (1999). Urbanization and state formation. In Companion Encyclopedia of Archaeology, *Volume 1-2*, G. Barker, ed. (Routledge), pp. 908–949.

90. Wiersma, C.W. (2020). House (centric) societies on the prehistoric Greek mainland. Oxf. J. Archaeol. *39*, 141–158.

91. I. Kuijt, ed. (2000). Life in Neolithic Farming Communities: Social Organization, Identity, and Differentiation (Kluwer Academic Publishers).

92. Porčić, M. (2012). Social complexity and inequality in the Late Neolithic of the Central Balkans: Reviewing the evidence. Documenta Praehistorica *39*, 167–183.

93. Timothy, E. (2011). Chiefs, chieftaincies, chiefdoms, and chiefly confederacies: power in the evolution of political systems. Soc. Evol. Hist. *10*, 27–54.

94. B. Hanks, and K. Linduff, eds. (2009). Social Complexity in Prehistoric Eurasia: Monuments, Metals and Mobility (Cambridge University Press).

95. Ur, J. (2014). Households and the emergence of cities in Ancient Mesopotamia. Camb. Archaeol. J. *24*, 249–268.

96. Barjamovic, G. (2013). Mesopotamian empires. In The Oxford handbook of the state in the Ancient Near East and Mediterranean, , W. Scheidel, ed. (Oxford University Press), pp. 120–160.

97. Kradin, N.N. (2019). Social complexity, inner Asia, and pastoral nomadism. Soc. Evol. Hist. *18*, 3–34.

98. Fu, Q., Li, H., Moorjani, P., Jay, F., Slepchenko, S.M., Bondarev, A.A., Johnson, P.L.F., Aximu-Petri, A., Prüfer, K., de Filippo, C., et al. (2014). Genome sequence of a 45,000-year-old modern human from western Siberia. Nature *514*, 445–449.

99. Peter, B.M., Petkova, D., and Novembre, J. (2020). Genetic landscapes reveal how human genetic diversity aligns with geography. Mol. Biol. Evol. *37*, 943–951.

100. Fu, Q., Meyer, M., Gao, X., Stenzel, U., Burbano, H.A., Kelso, J., and Pääbo, S. (2013). DNA analysis of an early modern human from Tianyuan Cave, China. Proc. Natl. Acad. Sci. USA *110*, 2223–2227.

101. Knaus, B.J., and Grünwald, N.J. (2017). vcfr: a package to manipulate and visualize variant call format data in R. Mol. Ecol. Resour. *17*, 44–53.

102. Bergström, A., McCarthy, S.A., Hui, R., Almarri, M.A., Ayub, Q., Danecek, P., Chen, Y., Felkel, S., Hallast, P., Kamm, J., et al. (2020). Insights into human genetic variation and population history from 929 diverse genomes. Science *367*, eaay5012.

103. Hinrichs, A.S., Karolchik, D., Baertsch, R., Barber, G.P., Bejerano, G., Clawson, H., Diekhans, M., Furey, T.S., Harte, R.A., Hsu, F., et al. (2006). The UCSC Genome Browser Database: update 2006. Nucleic Acids Res. *34*, D590–D598.

104. R Core Team (2019). R: A Language and Environment for Statistical Computing. (The R Project for Statistical Computing).

105. Briggs, A.W., Stenzel, U., Johnson, P.L.F., Green, R.E., Kelso, J., Prüfer, K., Meyer, M., Krause, J., Ronan, M.T., Lachmann, M., et al. (2007). Patterns of damage in genomic DNA sequences from a Neandertal. Proc. Natl. Acad. Sci. U S A *104*, 14616–14621.

106. Lawrence, M., Huber, W., Pagès, H., Aboyoun, P., Carlson, M., Gentleman, R., Morgan, M.T., and Carey, V.J. (2013). Software for computing and annotating genomic ranges. PLoS Comput. Biol. *9*, e1003118.

107. Pebesma, E.J. (2004). Multivariable geostatistics in S: The gstat package. Comput. Geosci. *30*, 683–691.

108. Jacquard, A. (1975). Inbreeding: one word, several meanings. Theor. Popul. Biol. *7*, 338–363.

109. Weir, B.S. (2012). Estimating F-statistics: A historical view. Philos. Sci. *79*, 637–643.

STAR★METHODS

KEY RESOURCES TABLE

REAGENT or RESOURCE	SOURCE	IDENTIFIER
Deposited data		
Processed genotype data (vcf files)	This study	https://doi.org/10.5281/zenodo.4906173
Software and algorithms		
Burrows-Wheeler Aligner BWA aln 0.7.15	[69]	http://bio-bwa.sourceforge.net/
SAMtools-0.1.19	[70]	https://github.com/samtools/samtools
FilterUniqueSAMCons.py	[71]	https://bioinf.eva.mpg.de/fastqProcessing/
bamUtil	[72]	https://github.com/statgen/bamUtil
Bcftools	[73]	https://samtools.github.io/bcftools/
PLINK v1.9	[74,75]	https://www.cog-genomics.org/plink2
modifyfasta.py	This study	https://github.com/CompEvoMetu/ROH
Gargammel	[76]	https://github.com/grenaud/gargammel
PED-SIM	[77]	https://github.com/williamslab/ped-sim
Msprime	[78]	https://github.com/tskit-dev/msprime
Other		
Custom code for analyses	This study	https://doi.org/10.5281/zenodo.4906173

RESOURCE AVAILABILITY

Lead contact

Further information and requests for resources and reagents should be directed to and will be fulfilled by the Lead Contact: Mehmet Somel (msomel@metu.edu.tr).

Materials availability

This study did not generate new unique reagents.

Data and code availability

The processed ancient genome data (VCF files) used in this study and the supplemental data tables (Data S1, S2, and S3) are deposited at Zenodo and are publicly available as of the date of publication. The DOI is listed in the key resources table.

The computer simulation codes, bash scripts and the R code used in the study have been deposited at Zenodo and are publicly available as of the date of publication. The DOI is listed in the key resources table. All original code is also available at https://github.com/CompEvoMetu/ROH.

Any additional information required to reanalyze the data reported in this paper is available from the lead contact upon request.

EXPERIMENTAL MODEL AND SUBJECT DETAILS

Classification into broad cultural groups

Identifying social complexity in archaeology is an issue in itself, and the debate in archaeology and cultural anthropology still continues.[79–82] Social complexity can be defined as increased differences in status that leads to social hierarchies in control of economic and social activities by a centralized agent and its bureaucratic devices, such as a chief or a state.[83] Archaeological correlates to this phenomenon include increased population size as demonstrated in settlement patterns, complex organization of labor as demonstrated in labor intensive subsistence activities and architectural projects, social networks as demonstrated in long-distance exchange of artifacts and raw materials, or intensified and elaborated ritual activities.[84] Here, we use a fourfold division that corresponds to some of the most important socio-economic thresholds in human (pre)history.

Hunter-gatherer groups are small-scale egalitarian mobile bands that subsist by utilizing the wild resources. While some hunter-gatherer communities can be involved in long-distance exchange, elaborate ritual, and labor control for large scale architectural projects,[85] the emergent complexity is often fragile in the absence of storage and redistributive mechanisms.[86] In these groups, often the accumulation of wealth by individuals or certain groups as well as transference of acquired status to kin members are not permitted.

Prior to the Holocene, hunting-gathering-foraging was the sole source of livelihood; however, with the onset of the Holocene, long term sedentism and intensification of animal and plant management gave way to domestication and the establishment of agricultural societies, i.e., the Neolithic Process.[87] It is understood that the advent of agriculture is the basis for more solid forms of social complexity, particularly due to the emergence of a new social and economic organization that this pattern of subsistence requires. In particular, the increase in population sizes, the emergence of storage and redistribution mechanisms, along with a new social and economic organization that is focused on competing households and extended kinship networks, seem to have resulted in more complex forms of social organization, such as chiefdoms and states.[88–90] In these societies, competing groups seek to expand their labor force within a kinship making system, which can be secured by marriage alliances with a wide range of groups; in this context, prestigious families attract more alliances and multiple spouses can be attained.

For our purposes, we identified three types of past agriculturalist societies in Eurasia. We chose to name the early sedentary agricultural villages without a centralized institution that is at the top of a hierarchical social organization as simple agriculturalists, in any geographical area.[91,92] These societies represent the earliest farming groups in their region, either growing organically from the preceding hunter-gatherer groups, or through a process of drawn-out interaction and/or replacement by pre-existing farmer communities. Second, the groups that show forms of incipient centralization and institutionalized hierarchy are named early complex agriculturalists, indicating a degree of social complexity as particularly evidenced in their ritual activity, settlement pattern, architecture and craft specialization.[45,46,93–95] These include those societies caught in the process of urbanization, early metal-working societies, and pastoral groups that eventually boosted their mobility with the domestication of the horse. Lastly, the advanced complex agriculturalists include the highly stratified societies organized around states, depending on a system of economical accumulation and redistribution based on a formal, typically hereditary leadership.[47,96,97]

Grouped in this way, the periodization that we apply to past societies is not a universal and time-dependent evolutionary scheme, but is rather a function of historical developments unique to each region that resulted in different responses. Data S1C and Figure S3F provide a description of the rough initiation dates of each cultural group in each of the two regions of Eurasia.

METHOD DETAILS

Overview of the genome data

We made use of the rich collection of published ancient genomes in this study. We built two different ancient genome datasets. The first was used for method development, and included n = 44 ancient genomes with coverages higher than 10x. These were used to optimize ROH calling to suit ancient genomes with different coverage (Data S1E).[5–7,9–20,98] Once having determined that our approach yielded unbiased ROH estimates with genomes with coverage > 3x, we built a second dataset to study the evolution of autozygosity during the Holocene. We limited our sample to genomes of the last 15,000 years, and also to West and Central Eurasia; this spatiotemporal frame contains the highest density of published ancient genomes, providing sufficient power to test our hypotheses on change in inbreeding patterns over time. The second dataset thus contained n = 411 ancient genomes that met at least one of these two criteria: they had $\geq$3x mean SNP coverage across the 1240K SNP set irrespective of missingness (n = 404) or had $\geq$2x coverage and less than 30% missing SNPs overall (n = 7) (Data S1B).[5–34] The distribution of coverage and missingness levels across these genomes are shown in Figures S2E and S2F. We note that we were motivated to include the latter small group of 7 genomes with $\geq$2x coverage because it included a historically interesting genome with extreme levels of autozygosity (Chan); meanwhile removing these 7 individuals does not alter any of our main results. We also performed additional controls to ensure that variance in coverage and missingness does not influence our analyses, e.g., we included coverage and missingness as explanatory variables in multiple regression models of FROH (see below).

Figures S3C–S3F shows the temporal distribution of the genomes collected, ranging between 520 CE and 12,030 BCE. Further, to study the effects of sociocultural organization and economic activity, we divided ancient West and Central Eurasians into four cultural groupings, according to the chronological periodization scheme described earlier (see "Classification into broad cultural groups"). These included: hunter-gatherers (n = 40), simple agriculturalists (n = 102), early complex agriculturalists (n = 230) and advanced complex agriculturalists (n = 39). For comparison purposes we also analyzed 19 West and Central Eurasian populations from the Human Genome Diversity Panel (HGDP) with n = 448 present-day individuals in total (Data S1F).

The spatial distribution of ancient and present-day individuals is shown in Figures S3A and S3B. We divided our focal region of Eurasia into two, in order to study possible spatial patterns. We used the Aegean, the Black Sea, the Caucasus and the Urals to delineate West and Central Eurasia. Individuals belonging to the west of this demarcation line were considered West Eurasians (n = 275 ancient and n = 155 modern) and individuals belonging to the east of the line, Central Eurasians (n = 136 ancient and n = 293 modern). This demarcation overlaps with major geographical boundaries that appear to have hindered population contacts.[99] Finally, we use two outbred populations, African ancestry from Barbados in the Caribbean (ACB) and African ancestry in Southwest USA (ASW) from the 1000 Genomes dataset,[56] to define a baseline to compare the number and sum of ROH in Figure 3.

QUANTIFICATION AND STATISTICAL ANALYSIS

Processing ancient genome data

We downloaded published ancient human genomes produced in various studies, listed in Data S1B and S1E. These included data obtained by shotgun sequencing or DNA target-enrichment of 1.24 million genome-wide single-nucleotide polymorphisms (SNPs)

(the so-called "1240k capture" process).[6,19,100] To decrease bias resulting from different pipelines in the original studies, we processed all the raw data through our own pipeline. First, we mapped the reads to the human reference genome (hs37d5) using the Burrows–Wheeler Aligner (*BWA*, v. 0.7.15),[69] with parameters '-l 16500, -n 0.01, -o 2'. Then we used *SAMtools "merge"* (v. 1.9)[70] to merge all libraries from the same individual and removed PCR duplicates using *FilterUniqueSAMCons.py*.[71] We removed reads shorter than 35 base pairs and those with > 10% mismatches to the reference genome. We trimmed the BAM files of the ancient individuals to remove postmortem damage-caused mismatches at the read ends, in order to avoid interpreting these as true variants. We trimmed reads from both ends by 10 bp if no UDG treatment was used in the original study, and 2 bp if the samples were UDG-treated, using the trimBAM command of the *bamUtil* software.[72]

For genotyping we used the 1240k SNP panel as reference and its subset of 1,151,161 autosomal SNPs. We used *SAMtools mpileup* to call genotypes of ancient individuals using this panel (parameters: '-B -q30 -Q30').[6] The output BCF files were converted to VCF files with parameters '-mV indels' using the bcftools call command.[73] We obtained the mean coverage per genome across the 1240K SNP set by collecting SNP read depths from each VCF file (i.e., the 'DP' field), also accounting for missing SNPs for each genome using the R package *VcfR v1.12*.[101] This is the coverage value we report throughout this study for all samples. Finally, the VCF files were converted to *PLINK* input files using *PLINK* v1.9.[74,75]

In order to ensure that our results are robust to the choice of reference SNP panel, SNP density, and confounding by postmortem damage, we further repeated the analyses using a denser Yoruba transversion SNP panel (> 1.9 million SNPs) from the phase 3 of 1000 Genomes Project[52] (see "The effect of using a denser SNP panel" below).

Processing modern-day genome data. In parallel with ancient genomes, we also analyzed n = 448 individuals from the Human Genome Diversity Panel (HGDP) (belonging to 19 populations)[102] and n = 235 admixed (outbred) individuals from the 1000 Genomes (belonging to two populations: ASW and ACB).[56] We used the version 3.0 of the HGDP which consists of high coverage WGS data (data obtained from ftp://ngs.sanger.ac.uk:21/production/hgdp/hgdp_wgs.20190516) and genotype data (Illumina BedStation and Infinium Omni 2.5) from the 1K Genomes individuals (data obtained from http://ftp.1000genomes.ebi.ac.uk/vol1/ftp/release/20130502). We filtered both HGDP and 1K Genomes individuals using the 1240k SNP panel so that the genotypes of all the individuals in this study were based on the same SNP panel. Since HGDP data is based on the GRCh38 reference genome, but 1240K is based on GRCh37, a liftover to the HGDP dataset was applied.[103]

Statistical analyses

All statistical tests and procedures described below were performed using *R* v3.6.1.[104] All hypothesis testing was conducted two-sided.

ROH calling procedures

We used *PLINK v1.9*[74,75] to identify ROH. *PLINK* has been extensively used to call ROH in human genomic studies and is the most widely used software for this purpose.[37] We chose *PLINK* due to its methodological convenience: its direct observational approach allows the researcher to have full control of the ROH calling process. Also, by modifying *PLINK* parameters, it has been shown that it is possible to obtain equivalent ROH estimations between different sequencing technologies and genomic coverages.[37]

ROH were called in autosomes with the following arguments:

–*homozyg-snp 30.* Minimum number of SNPs that a ROH is required to contain (30 SNPs).

–*homozyg-kb 500.* Length in Kb of the sliding window (500 Kb).

–*homozyg-density 30.* Required minimum density to consider a ROH (1 SNP in 30 Kb).

–*homozyg-gap 1000.* Length in Kb between two SNPs to be considered in two different segments (1 Mb).

–*homozyg-window-snp 30.* Number of SNPs that the sliding window must contain (30 SNPs).

–*homozyg-window-het (0 - 1).* Number of heterozygous SNPs allowed in a window (0 or 1).

–*homozyg-window-missing 5.* Number of missing calls allowed in a window (5 calls).

–*homozyg-window-threshold 0.05.* Proportion of overlapping windows that must be called homozygous to define a given SNP as within a "homozygous" segment (5%).

We collected the following statistics on the total number of ROH events (NROH) or the total sum of ROH events (SROH) from the outcome file of each *PLINK* run:

- NROH for ROH longer than 1 Mb ($NROH_{>1Mb}$), longer than 1.5 Mb ($NROH_{>1.5Mb}$), or shorter than 1 Mb ($NROH_{<1Mb}$),
- SROH for ROH longer than 1 Mb ($SROH_{>1Mb}$), longer than 1.5 Mb ($SROH_{>1.5Mb}$), or shorter than 1 Mb ($SROH_{<1Mb}$),
- $SROH_{>1.5Mb}$ divided by the total length of the autosomal genome, which is used to estimate the genomic inbreeding coefficient, F_{ROH}.[51]

On each genome we estimated ROH using *PLINK* in two ways, allowing no heterozygous SNP per window ('het 0'), and allowing one heterozygous SNP ('het 1').

Simulating ancient genomes with spiked-in ROH

We tested the performance of our *PLINK*-based approach and also our conditional scheme (described below) using purely simulated data. First, we created simulated genotypes with ROH of different numbers and sizes on human Chromosome 1 (chr1), using the 1240K SNP list.[6] We created ROH under two different scenarios (see below), each with 20 individuals, and each at three different genome coverages: 3x, 5x, and 10x. Each individual's diploid chr1 was created as follows in the R environment (*R* v4).

1) Creating outbred chromosomes: (a) We chose a single random allele at each of the 1240K SNPs on chr1 (n = 93,207 SNPs), (b) we chose the alternative allele as second allele of that individual's genotype with 10% probability (i.e., we chose the same allele with

90% probability). This approximates realistic heterozygosity levels at 1240K SNP positions on chr1 among the Eurasian ancient genomes we analyzed (c.12%).

2) Spiking in ROHs of different size: Artificial 1 Mb ROHs were then randomly inserted into each such simulated chr1 bed file. This we performed by converting all heterozygous positions within that stretch to homozygous state. Under scenario 1, we inserted 2 × 1 Mb ROH per individual, under scenario 2 we inserted 10 × 1 Mb ROH per individual. In the simulations we ensured that randomly inserted ROH were separated by at least 1.5 Mb to avoid spiked-in ROH overlaps and the generation of extra-long ROH. We also ensured that ROH were not inserted in the 23 Mb centromeric region of chr1, which is devoid of 1240K SNPs. Using each simulated bed file, we then created a chr1 fasta file using a custom *Python* script ''modifyfasta.'' The custom *R* and *Python* scripts for these steps are available at GitHub (https://github.com/CompEvoMetu/ROH).

3) Creating ancient reads: The fasta files were in turn used as input to create simulated aDNA reads with the *gargammel* software.[76] This included the generation of reads, with average read length set to 70 bp, and simulation of postmortem damage, i.e., deamination-caused C->T and G->A transitions at read ends. The Briggs model parameters were used for postmortem damage simulation.[105] For each of the 20 simulated individuals and for each scenario, we created 20.9, 35.6, and 71.2 million chr1 reads on average, for coverages 3x, 5x, and 10x, respectively.

After adapter removal, all simulated reads were then processed using the same pipeline as used in the original data analysis (see ''Processing ancient genome data'' above): reads were trimmed for 10 bp from both ends, aligned to the reference genome, SNPs were called with *SAMtools mpileup* and the 1240K SNP panel, and ROH were called using *PLINK* with the same parameters, including allowing either 0 or 1 heterozygous SNP per window.

We also analyzed the effect of missing SNPs using the same simulated data. For this, we randomly removed 30% of the SNPs from each simulated chromosome in *R* v4, before performing ROH calling.

Analyzing spiked-in ROH simulation results

We assessed the performance of our ROH calling approach on low coverage data using spiked-in ROH in simulated chr1 data (described in the previous section). We measured recall and false discovery rate (FDR), as well as deviation of estimated $NROH_{>1Mb}$ and $SROH_{>1Mb}$ values from expected.

To determine the true and false positives, we used the *R* package *GenomicRanges v1.12.5*[106]. True positives were defined as ROH that showed > 90% overlap between expected and observed ROH positions, and that strictly reached 1 Mb length. False positives were defined as ROH that did not fulfil the above criteria.

Using the *PLINK* 'het = 1' parameter for ROH calling, recall rates were promisingly > 90% in both scenarios and at all coverages (Data S1G). Meanwhile, FDR varied from 0.04 to 0.61, with the highest rates observed at 3x. The elevation in FDR at low coverage is expected: the lower the coverage, the higher the fraction of heterozygous sites missed due to sampling error (see ''Applying the ROH estimation scheme'' below).

For coverages 5x and 10x, *NROH* and *SROH* estimates were close to expected values. Under scenario 1, for *SROH* estimates the median deviation from expected values was 21% and the full range was [4%–138%], and for *NROH* estimates the median was 0% [0%–100%]. Under scenario 2, for *SROH* estimates the median deviation was 17% [0%–32%], and for *NROH* estimates the median was 0% [0%–20%] (Data S1A and S1H).

At 3x coverage calculated with the ''het 1'' parameter, we observed greater deviations from expected values. Under scenario 1, for *SROH* estimates the median deviation was 185% [64%–465%], and for *NROH* estimates the median was 150% [50%–350%]. Under scenario 2, for *SROH* estimates the median deviation was 59% [20%–100%], and for *NROH* estimates the median was 30% [0%–50%].

As described below, we found that using the ''het 0.5'' correction improves these results (see ''Applying the ROH estimation scheme'' below).

Downsampling simulations

We next studied the effect of genome coverage on ROH calling using simulations with real ancient genome data. For this, we simulated low coverage genomes by downsampling the n = 44 ancient genomes with > 10x coverage (Data S1E). We used *Picard*'s *DownsampleSam* tool (https://broadinstitute.github.io/picard) to randomly extract reads from BAM files to obtain 10x, 5x, 3x and 2x coverage versions. We thus created 10x, 5x, 3x and 2x versions for each ancient genome, yielding a total of n = 220 full or partial genomes. Table S1 shows variant calling results across coverages. This reveals that with lower genome coverages, there arises a bias towards calling homozygous genotypes over heterozygous genotypes, as expected due to sampling error. Consequently, low coverage leads to systematic overestimation of the sum of ROHs with *PLINK* (Figure S1).

The 'het 0.5' correction

As Figure S1 shows, at genome coverages < 5x, *PLINK* overestimates ROH. Conversely, allowing using 'het 0' instead of 'het 1' (i.e., not allowing heterozygous SNPs per window) leads to underestimation of ROH. This is also consistent with our observations using spiked-in ROH in simulated ancient genomes (Data S1G). Studying the results of downsampling simulations using real genomes, we observed that the two effects can partly cancel each other out at 3x coverage. Specifically, when we calculated the average between the 'het 0' estimate and the 'het 1' estimate for various statistics ($NROH_{>1Mb}$, $NROH_{<1Mb}$, $SROH_{>1Mb}$, $SROH_{<1Mb}$, F_{ROH}), we found that the averages empirically approximate the original estimates at high coverage (explained below). We refer to this approach,

i.e. estimating ROH statistics for low coverage genomes as an average between two estimates as the "'het 0.5' correction" (Figure S1). For instance, the 'het 0.5' corrected estimate for $SROH_{>1Mb}$ is the average between $SROH_{>1Mb}$ calculated using 'het 0' and $SROH_{>1Mb}$ calculated using 'het 1'.

A conditional ROH estimation scheme

We hypothesized that we could limit the effect of coverage on ROH calls by conditioning ROH calling parameters on coverage. We chose the number of heterozygous SNPs allowed per window depending on coverage: (a) for genomes with average genomic coverage $\geq$4x we allowed one heterozygous SNP per window (i.e., called ROH using 'het 1'), (b) for genomes with average genomic coverage < 4x we used the 'het 0.5' correction. We chose 4x as the midway between two values: when using 'het 1', at 5x we observe negligible deviation from expected *SROH* values when downsampling real ancient genomes and also in spike-in simulations, whereas at 3x coverage the deviation becomes conspicuous.

Testing the ROH estimation scheme

To assess the effects of different genomic coverage on ROH measurements, we estimated ROH using different approaches, and then studied the outcomes with regression analyses. Here we made use of the downsampling simulation dataset based on the 44 ancient high coverage genomes introduced earlier.

First, we calculated ROH using the 'het 0', 'het 1' and 'het 0.5' schemes on all 44 ancient genomes. We then tested the effects of coverage and ROH calling scheme by fitting the below general linear model, which we call model 1:

$$Y_{ijk} = \gamma_{00} + C_i + V_j + U_k, \quad (1)$$

where Y_{ijk} is the response variable (either $NROH_{>1Mb}$, $NROH_{<1Mb}$, $SROH_{>1Mb}$, or $SROH_{<1Mb}$) with coverage *i*, the number heterozygous SNPs allowed per window *j,* and the individual (as random effect) *k.* Here, γ_{00} is the overall mean, C_i is the fixed effect of the genomic coverage of each individual (n = 5 types: full, 10x, 5x, 3x and 2x), V_j is the fixed effect of the number of heterozygous SNPs allowed per window (n = 3 types: 'het 0', 'het 1' and 'het 0.5') and U_k is the random effect of the individual (n = 44). This regression was repeated separately for each of the four response variables.

Second, we used the conditional scheme, where we estimated ROH using 'het 1' for genomes with average genomic coverage $\geq$4x and using the 'het 0.5' correction for genomes with average genomic coverage < 4x. We then fit the following general linear model, which we call model 2:

$$Y_{ik} = \gamma_{00} + C_i + U_k, \quad (2)$$

where Y_{ik} is the response variable (either $NROH_{>1Mb}$, $NROH_{<1Mb}$, $SROH_{>1Mb}$, or $SROH_{<1Mb}$) with coverage *i,* and individual (as random effect) *k.* Here, γ_{00} is the overall mean, C_i is the fixed effect of the genomic coverage of each individual (n = 5 types: full, 10x, 5x, 3x and 2x), and U_k is the random effect of the individual (n = 44).

The results of both models (1) and (2) are shown in Data S2. We found that the coverage effect was highly significant ($p < 2.2e-16$) in both trials. However, when the different coverage classes (> 10x, 10x, 5x, 3x and 2x) are pairwise compared (Figures S3G–S3J; Data S2) we can see that, by using the conditional scheme, it is possible to obtain statistically non-different estimations of $NROH_{>1Mb}$ and for $SROH_{>1Mb}$ for average genomic coverage down to 3x.

We also found that for ROH < 1Mb, none of these approaches could remove the effect of variable genomic coverage on ROH calls, i.e., $NROH_{<1Mb}$ and $SROH_{<1Mb}$ statistics (data not shown).

Applying the ROH estimation scheme

We further investigated the performance of our conditional ROH estimation approach using the spiked-in ROH dataset (see above). We used the 'het 0.5' correction for simulated genomes with 3x coverage, and used 'het 1' for simulated genomes with 5x or 10x coverage (Figures S2A and S2B).

For the comparison of 3x ('het 0.5') results with those of 3x ('het 1'), we first studied the simulations without missing data. When calling ROH (1 Mb) using 'het 0.5' at 3x coverage, *NROH* and *SROH* values showed systematically lower deviation. Specifically, for scenario 1, *SROH* median deviation was 43% with a full range of [4%–182%], and *NROH* median deviation was 25% [0%–125%]; under scenario 2, *SROH* median deviation was 5% [4%–34%], and *NROH* median deviation was 25% [0%–45%]. In comparison, using 'het 1' at 3x coverage, under scenario 1, we had observed the following: for *SROH* median deviation was 185% [64%–465%], for *NROH* 150% [50%–350%]; under scenario 2, for *SROH* median deviation was 59% [20%–100%], and for *NROH* 30% [0%–50%]. We thus find considerable improvement using 'het 0.5', especially on *SROH* estimates.

We also repeated this analysis after inserting 30% missing data. We once again detected lower deviations using 'het 0.5' (for scenario 1, *SROH* median deviation was 246% with a full range of [83%–390%], and *NROH* median deviation was 175% [50%–300%], and for scenario 2, *SROH* median deviation was 37% [2%–62%], and *NROH* median deviation was 5% [0%–35%]), compared to deviations found using the 'het 1' parameter (for scenario 1, *SROH* median deviation 572% [249%–879%], *NROH* median 425% [200%–700%], and for scenario 2, *SROH* median deviation was 121% [72%–190%], and *NROH* median 75% [30%–120%]).

We then visualized F_{ROH} values estimated in the simulated dataset using the conditional approach; here F_{ROH} was calculated as *SROH* $\geq$1Mb divided by the chromosome size (Figure S2A).

Importantly, using our conditional approach for ROH estimation, the deviations we find in the spike-in simulation experiment in ROH estimates (e.g., F_{ROH} with 1 Mb), at either 3x, 5x and 10x coverages, (e.g., F_{ROH} median deviation 0-0.016, with a mean of 0.005) were of much smaller magnitude than F_{ROH} variation within the real ancient sample we are studying (F_{ROH} ranging between 0.0004-0.23 with a mean of 0.031; see Figure 1A).

F_{ROH} measurements and consanguinity

In view of our downsampling experiments and the regression analysis results, in downstream analyses we used the genomic inbreeding coefficient, or F_{ROH} (sum of ROH > 1.5 Mb)[51] calculated using our conditional approach: i.e., using 'het 1' for genomes $\geq$4x coverage, and 'het 0.5' scheme for genomes between 3x to 4x coverage.

We used different F_{ROH} thresholds to define different consanguinity matings (Table 1). F_{ROH} > 0.0117 (average value between the genealogical inbreeding coefficient of second and third cousin) designates individuals who could be the offspring of a second cousin marriage. F_{ROH} > 0.039 (average value between the genealogical inbreeding coefficient of first and second cousin) designates individuals who could be the offspring of a first cousin marriage. F_{ROH} > 0.093 (average value between the genealogical inbreeding coefficient of first and avuncular mating) designates individuals who could be the offspring of an avuncular marriage. All estimates ignore drift.

Temporal and spatial distribution of F_{ROH}

We used different approaches to assess the effect of temporal and spatial distribution in F_{ROH} of the individuals analyzed in this study. We first fit a simple regression analysis of F_{ROH} on the archaeological time of ancient individuals (Figure 1). We also compared among different cultural groupings using a Wilcoxon pairwise rank-sum test with continuity correction using the *R* 'wilcox.test' function. We further fit a multiple regression model with both the archaeological time and cultural grouping (Data S3, also see "Testing the effects of varying coverage" below). To test the spatial distribution, we first fit a multiple regression analysis with F_{ROH} as dependent variable, and the longitude, latitude, and archaeological time of each ancient individual as independent variables. To delve deeper in the spatial distribution of the F_{ROH}, we divided the complete dataset into the designed cultural groupings, and we fitted a kriging, or Gaussian process regression, using the functions *variogram()*, *fit.variogram()* and *krige()* in R package *Gstat v2.06*.[107] To obtain the variogram we used an exponential model.

Studying the origins of autozygosity

Two distinct and independent biological scenarios can increase homozygosity in natural populations: cultural consanguinity and genetic drift in isolated populations. These two different sources were defined in classical population genetics as systematic inbreeding (denoted by F_{IS}) and panmictic inbreeding (denoted by F_{ST}), respectively.[53,108] Total inbreeding, denoted by F_{IT}, is defined by $(1\text{-}F_{IT}) = (1\text{-}F_{IS})\ (1\text{-}F_{ST})$.[109]

Panmictic inbreeding occurs in isolated populations, when individuals randomly mate within their own group, with no immigration. Population isolation can be cultural, a consequence of geographical barriers or because of sedentary behavior. Importantly, isolation by itself does not create genomic autozygosity, except when the effective population size (N_e) is small and genetic drift has the strength to remove genetic variability. On the other hand, systematic inbreeding, or cultural consanguinity, has the effect of reducing heterozygosity relative to the expectation under Hardy-Weinberg equilibrium independent of N_e, and thus increasing F_{IS}. High consanguinity (and consequent high F_{IS}), and genetic drift by isolation coupled with low N_e (and consequent high F_{ST}) are two independent and non-mutually-exclusive phenomena that can increase overall autozygosity (F_{IT}) in a population.

Here we also note that the term "endogamy" is generally used to describe population isolation, although the term is sometimes used to refer to consanguinity. To avoid confusion, we chose to avoid use of "endogamy" in the text.

Because we yet lack reliable estimates of population allele frequencies for these ancient populations, we cannot estimate F_{IS} and F_{ST} directly in this study. Instead, we may assess the origins of the autozygosity in our ancient genomes using comparisons of $NROH_{>1.5Mb}$ and $SROH_{>1.5Mb}$, as explained in Ceballos et al.[54] Namely, if an individual displays excess of $SROH_{>1.5Mb}$ relative to $NROH_{>1.5Mb}$ in comparison to non-consanguineous individuals, this suggests autozygosity by consanguinity. If both $SROH_{>1.5Mb}$ and $NROH_{>1.5Mb}$ are high, this suggests drift-driven autozygosity. This approach does not provide a quantitative estimation of the relative contributions of drift versus consanguinity, but only a qualitative assessment. Nevertheless, it is a powerful approach: its inferences on autozygosity patterns in modern human populations' genomes are consistent with known ethnographic data about consanguineous traditions, and about population size and isolation.[54]

Consanguinity and genetic drift simulations

In our study we estimated $NROH_{>1.5Mb}$ and $SROH_{>1.5Mb}$ using the conditional scheme across the 411 ancient genomes, and compared the two values (Figure 3A). We further performed three additional analyses to place our results in context.

First, we performed a simple pedigree simulation. We used an inhouse *R* script to simulate meioses using the GRCh37 genetic map downloaded from the UCSC Genome Browser (https://genome.ucsc.edu) under different levels of consanguineous mating, keeping track of break points, and recording consequent $NROH_{>1.5Mb}$ and $SROH_{>1.5Mb}$. We thus simulated ROH for 20,000 second cousin matings, first cousin matings, avuncular (uncle - niece, aunt - nephew, or double first cousin) matings, and incest (brother - sister, parent - offspring) matings (5,000 each) (Figure 3B). This simulation does not account for drift. However, in light of the earlier discussion about the independent effects of drift and consanguinity, we predicted that the degree of right shift should be projectable in cases where there exists a non-0 level of autozygosity due to drift.

We further sought to detect the possible effect of drift (panmictic inbreeding) when it is combined with the effect of systematic inbreeding using another set of simulations. For this, we used real data from two populations with different population histories: a sample of individuals with African ancestry in Southwest USA (ASW, n = 61), and Southern Han Chinese from China (CHS, n = 105), from the 1000 Genomes dataset. Using these two datasets, we again simulated second cousin, first cousin, avuncular and incest matings using the GRCh37 genetic map. This time we used the software *PED-SIM*[77] to create > 100 pedigrees for both populations. We specified the number of founders needed for each mating type in the DEF file (e.g., four founders for the inbreeding of first cousins). Given the set of individuals at hand, we could create 15 samples at each run (i.e., a total of 60 founders were required for first cousins at each run). We repeated the process until at least 100 samples were produced for each mating type (i.e., seven times for first cousins). Each time the founders were randomly chosen from the given file (n = 105 1st cousins, n = 100 2nd cousins, n = 100 avuncular and n = 100 incest matings in simulated ASW pedigrees, and n = 100 1st cousins, n = 105 2nd cousins, n = 105 avuncular and n = 105 incest matings in simulated CHS pedigrees). The *PED-SIM* parameters were '–pois–miss_rate 0–keep_phase' (i.e., using a Poisson crossover model, having no missing genotypes, and keeping the output phased). The VCF files containing the 1240K SNPs were converted to *PLINK* files and ROH were called using *PLINK* with the same parameters used throughout the study (Figure S2G).

Finally, we investigated the combined effect of genetic drift and consanguinity on $NROH_{>1.5Mb}$ and $SROH_{>1.5Mb}$ distributions by simulating data using a combination of coalescent simulations and pedigree simulations. To this end, we generated 100 human Chromosome 1 samples each for two hypothetical populations with effective population sizes (N_e) of 1000 and 10,000, again using the GRCh37 genetic map with *msprime*.[78] Then we used *PED-SIM*[77] to simulate mating between unrelated individuals, second cousin, first cousin, avuncular and incest matings for both hypothetical populations. This way, we created 112 second cousin, 100 first cousin, 132 avuncular, and 132 sibling matings using unrelated founders from the population with N_e = 1000, and 110 second cousin, 99 first cousin, 132 avuncular, and 132 sibling matings using unrelated founders from the population with N_e = 10,000. We called ROH from the *PED-SIM* output using the same *PLINK*-based approach as described above, with the 'het = 1' parameter. We note that even though we only used Chromosome 1 for this analysis for sake of time and memory, the resulting ROH values were consistent with those obtained using real ancient genomes (Figure S4). We observed the expected right-shifts in the NROH versus SROH plots, caused by increasing levels of consanguinity, and upward shifts caused by increasing drift (lower N_e). We further included NROH and SROH values estimated from Chromosome 1 in real ancient genomes in data visualizations. Two observations were notable: First, none of the individuals simulated under N_e = 1000 or N_e = 10,000 reached the NROH levels observed in the Chan individual from Mesolithic Spain. Second, a qualitative evaluation of the distribution of simulated NROH versus SROH values under drift and consanguinity again supported incest as the most likely scenario in the past of individual NG10 from Neolithic Ireland.

Testing the effects of varying coverage

We next sought to confirm that variation among samples in technical factors such as coverage and the proportion of missing SNPs does not influence our main conclusions.

First, we calculated whether $SROH_{>1.5Mb}$ (and F_{ROH}) or $NROH_{>1.5Mb}$ values were correlated with total coverage across all SNPs, coverage excluding missing SNPs (i.e., coverage across available SNPs), or missing SNP proportions (missingness) across the 411 ancient genomes. Note that the coverage value used throughout the study is total coverage across all 1240K SNPs, and is thus a measure that also reflects missingness.

NROH and *SROH* showed no correlation with coverage excluding missing SNPs (Kendall's rank correlation |tau|<0.06, p > 0.05), but they did show correlation with missingness and with total coverage (|tau|>0.13, p < 0.05) (Table S2). We also tested correlations between sample archaeological time (or sample age, in years BCE) and genome coverage or missingness. For missingness, there was no correlation (tau = −0.04, p = 0.23), while total coverage and coverage excluding missing SNPs and sample time showed weak correlations (|tau|>0.07, p < 0.05; Figure S3K; Table S2), with older genomes tending to have higher coverage.

We then asked whether these correlations between technical factors, sample time (age) and F_{ROH} may influence our main observation, that F_{ROH} levels decrease with time. For this, we first performed multiple regression analyses. F_{ROH} was the dependent variable, and sample archaeological time (age), cultural grouping, coverage (either total coverage or coverage excluding missing SNPs), and missingness, were independent variables.

In the full model (adjusted$v R^2$ = 0.32, p < 2.2e-16), only the sample archaeological time and cultural groupings were significant explanatory variables (p < 0.05), whereas coverage (excluding missing SNPs) or missingness had no significant contribution (p > 0.10) (Data S3). To validate this, we also compared a model with only archaeological time and cultural grouping as explanatory variables, with the full model. We found that including coverage and missingness in the model provided no significant improvement (ANOVA p = 0.31; Table S4). Repeating the same using total coverage qualitatively yielded the same results (Data S3).

Finally, we downsampled all genomes to the same coverage (3x). For this we again used *Picard*'s *DownsampleSam* tool (https://broadinstitute.github.io/picard) to randomly extract aligned reads from each BAM file in our full ancient dataset (n = 411). We thus obtained 3x average depth per SNP for all genomes, and repeated all analyses using these data. The results show that the whole dataset, when downsampled to the same minimum coverage, reveals the same main conclusions as the primary dataset used throughout the study (Figures S2I and S2J). Using the downsampled data, we detected the same correlation between the sample time and F_{ROH} (Pearson R^2 = 0.28, p < $2.2e^{-16}$) (Figure S2J). Furthermore, consanguinity practices in the previous generation were once again visible as a right shift in the *NROH* versus *SROH* comparison (e.g., for ancient individuals NG10, I6671 and I2521 on Figure S2I).

We further performed two additional analyses to rule out technical effects, described below.

Comparison with alternative approaches

Recently, two new model-based methods have been proposed to call ROH in ancient genomes. Renaud and colleagues (2019)[38] published *ROHan*, a Bayesian Hidden Markov Model (HMM) that co-estimates heterozygosity and ROH. *ROHan* was shown to accurately estimate ROH in ancient genomes with moderate damage with a coverage of at least 5x. A more recent study by Ringbauer et al.[39] reported *hapROH*, a method that makes use of a reference panel of phased haplotypes. *hapROH* uses an HMM to determine whether a stretch of pseudo-haploidized genotypes in an ancient genome systematically matches only a single haplotype in the panel, indicative of ROH in that region. With this additional information, Ringbauer et al.[39] report that *hapROH* can detect ROH > 4 cM in ancient DNA at much lower genome-wide coverage than earlier possible (> 0.3x).

Although *hapROH* is highly powerful for detecting ROH at coverages down to 0.3x, our approach has a number of relative advantages, including being model-free, its ease of implementation, its apparent power to detect ROH of lower size (down to 1 Mb), and not relying on genomic diversity panels. The latter point is probably the most important. Indeed, our *PLINK*-based conditional ROH estimation will be available for the study of inbreeding in non-model organisms where such panels are mostly absent. Even in humans, *hapROH*'s power depends on the linkage patterns of the populations in question, as demonstrated by its low power in African populations.

We compared the performance of our *PLINK*-based conditional ROH estimation scheme with that of *hapROH*[39] (data courtesy of Dr. Harald Ringbauer). We found that the *SROH* and *NROH* values for the n = 384 samples used in both studies and four different cultural groups (ROH > 4 cM; ROH > 8 cM; ROH > 12 cM; ROH > 20 cM) were highly similar. The *NROH* and *SROH* values of the two studies were correlated with Pearson $R^2 > 0.81$ for *NROH* and $R^2 > 0.89$ for *SROH* comparisons (Figures S2C and S2D). This strong consistency between our results, despite the difference in approaches, increases the reliability of both studies.

The effect of using a denser SNP panel

We repeated our main analyses using a second SNP panel. We chose a Yoruba transversion-only SNP panel (> 1.9 million SNPs) from the phase 3 of the 1000 Genomes Project, filtered for showing minor allele frequency > 10% in an African Yoruba sample.[52] We thus aimed to investigate the effects of different genomic densities of SNPs on our results, and to rule out any effect of residual postmortem damage (i.e., residual C->T transitions in ancient DNA reads that may not have been removed by trimming). We only included shotgun sequenced ancient genomes (n = 72; Data S1I), because the rest of the data (1240K capture genomes) would not include the bulk of the Yoruba panel SNPs.

We detected high correlation between F_{ROH} estimates obtained using the Yoruba SNP panel and 1240K SNP panel across the 72 shotgun ancient genomes (Figure S2H; Pearson $R^2 = 0.978$). This high consistency resonates with published results: Ceballos et al.[54] showed that $NROH_{>1Mb}$ and $SROH_{>1Mb}$ estimates from a dataset with 1.5M SNPs and from a whole genome sequencing dataset with more than 7M SNPs were highly similar. However, the same study also found that $NROH_{<1Mb}$ and $SROH_{<1Mb}$ estimates did vary with SNP density.